THERMAL TREATMENT OF PHOSPHOGYPSUM AS A SET RETARDER FOR PORTLAND CEMENT PRODUCTION

BY

AREMU, Gabriel Oluwatimilehin
MEng/SEET/2017/7011

DEPARTMENT OF CHEMICAL ENGINEERING
FEDERAL UNIVERSITY OF TECHNOLOGY
MINNA

OCTOBER, 2021

ABSTRACT

Photocatalytic degradation of simulated solution of tetracycline using plant mediated (phyto-enhanced) zinc oxide doped with graphitic carbon nitrite was investigated under solar light irradiation for 3 hours. Leaf extract from *Moringa oleifera* was the source of the phytochemical constituents used in the phyto-enhancement of zinc oxide synthesized by precipitation method using zinc nitrate precursor. Doping was achieved by physically mixing phyto-enhanced synthesized zinc oxide with graphitic carbon nitrite, a light yellow powder gotten from the calcination of melamine at 550 °C. The produced photocatalyst was characterized by FTIR, SEM-EDX, XRD and BET to determine the functional groups, structural morphology, elemental composition, crystallinity, surface area, pore volume and pore diameter. Doped phyto-enhanced zinc oxide showed evolved morphology, revealed loosed structure of uniformly distributed particles with increased surface area. This was confirmed by BET as the surface area (346.1 m^2/g) was 10 times greater than that of pure zinc oxide (35.44 m^2/g). The pore diameter and volume were 5.428 nm and 0.123 cm^3/g respectively compared to 2.965 nm and 0.01259 cm^3/g of pure zinc oxide. FTIR spectrum was recorded in the range of 4000–500 cm^{-1}. The FTIR result showed that Zn–O functional group was found at low wavenumber. The XRD pattern of doped phyto-enhanced zinc oxide nanoparticles showed that the substances only belong to ZnO although there were diffraction peaks of other impurities as a result of surface contamination and storage. The average crystallite size of the pure zinc oxide and the doped phyto-enhanced zinc oxide was estimated to be 29.87 nm and 30.27 nm respectively using Debye Scherer equation. The effective operation parameters employed to enhance the photocatalytic process are solution pH, initial concentration and catalyst dosage. The result showed that 98.7% degradation of tetracycline concentration of 5 mg/L was obtained with the optimum doping ratio of 5% (w/w), pH 8 and photocatalyst dosage of 0.2 g/L. This may be attributed to narrow band gab and improved electron/hole separation efficiency. Based on this outcome, it can be concluded that, phyto-enhanced zinc oxide doped with graphitic carbon nitrite photocatalyst can effectively degrade tetracycline in pharmaceutical effluents.

CHAPTER ONE

1.0 INTRODUCTION

1.1 Background to the Study

Cement is an inorganic silicate hydraulic binding material that is finely grounded from pulverized mixture of sintered clinker material, gypsum and other cementitious materials as additives. Cement is a hydraulic binder owing to the fact that it is water loving and reacts with water to give its binding property. It solidifies through hydration reactions and sticks to different materials to bind them together like sand and gravel (aggregates) to form concrete, which retains its stability and mechanical strength even under water (Oyenuga, 2014). According to Edwards (2011), cement is one of the key construction materials in use today; it is just behind water as the second most generally utilized material on the planet. Cement isn't typically utilized alone, but instead blended in with sand and rock (aggregate) to bind them together. Little amount of gypsum is added to the crushed clinker during the final milling of the cement manufacturing process to control the setting time for easy workability of the cement produced (Oyenuga, 2014).

Gypsum is a material that is broadly utilized in the cement industry, phosphogypsum (PG) on the other hand is typically not utilized, but is stored indefinitely in the light of the fact that through the wet procedure, some contaminants found in the phosphates rock which incorporates fluoride, sulphate, residual acidity, natural matter, heavy metals, sodium silicofluorides and phosphates becomes amassed in phosphogypsum which limit the compressive strength utilization of phosphogypsum in cement industry as a set retarder (Al-

Hwaiti *et al.*, 2013). The discharge of phosphogypsum into open terrain may pose environmental and health risks because the hazardous elements found in phosphogypsum trash landfills are constantly being released into the environment by climatic precipitation, potentially contaminating the topsoil and or groundwater. According to Abramov *et al* (2008), phosphogypsum takes longer time to set due to the phosphoric acid that retards the hydration process and decreases the compressive strength on immersion in water. This may affect work that needed immediate setting for further workability (Chen and Kwan, 2014).

Numerous studies have been conducted on phosphogypsum as a raw material for the manufacture of cement. The material has in this way, been attempted to fuse in concrete making due to its feasible use to control the hydration rate of reaction in regular Portland cement, phosphogypsum could be utilized as a substitute for natural gypsum in the manufacturing process (Ayres *et al.*,2001). The construction of phosphoric acid factories in areas where natural gypsum is scarce, the gradual exhaustion of gypsum quarries, and the struggle against water pollution have reignited interest in these studies (Van-Der-Merwe and Strydom, 2004).

Phosphogypsum cannot be utilized in its raw state on account of the impurities present in it, it ought to at first be exposed to a decontamination interaction process to eliminate those components which meddle with its setting or unfavorably influence the properties of the cement produced. The way toward purifying the phosphogypsum for the most part comprises of balance of the free corrosive, impregnating the gypsum and treatment by hydrocyclone, buoyancy, and twofold calcination (Oumnih *et al.*, 2017).

Thermal reaction of phosphogypsum containing calcium oxide with bentonite clay can give di-calcium silicates and tri-calcium silicates with perceived binding properties due to the materials binding possibility and properties gotten (Hammas-Nasri, 2016).

Currently, complete use of phosphogypsum resource is the most ideal approach to take care of the issue of phosphogypsum contamination, and the utilization of phosphogypsum binder preparation is the principle bearing of resource reutilization.

1.2 Statement of the Research Problem

Phosphogypsum consists of calcium sulphate ($CaSO_4$. $2H_2O$) and some impurities such as phosphoric oxide (P_2O_5), fluorine (F) and some organic substances. The presence of acidic admixtures phosphoric acid (H_3PO_4), hydrogen fluoride (HF), fluorosilicic acid (H_2SiF_6) does not allow to reuse this by-product for structural gypsum production without any reprocessing. Phosphoric acid (H_3PO_4) can retard the hydration process/setting time and decrease the compressive strength on immersion in water (Al-Hwaiti *et al*., 2013). These impurities seriously restrict the industrial use of phosphogypsum in cement industry as a retarder**.**

Dumping of phosphogypsum into open land takes a large span of land and could have environmental and health concerns. The stockpiled material dominated by calcium sulphate dihydrate contains impurities and toxic substances which can be transported by wind over long distances (Rashad, 2017). According to Kazragis (2004), good quality binding materials were not obtained when phosphogypsum was treated with slake lime water to obtain hemi hydrate gypsum due to the obstruction admixtures present in the phosphogypsum. In this research work, thermal treatment of phosphogypsum containing calcium oxide with acidic

oxides (bentonite) is introduced to decontaminate and remove the obstructive admixtures effectively with the production of tri-calcium silicates and di-calcium silicates with distinguished binding properties; and also analyze and compare the strength properties, paste-hardened microscopic body and microscopic as well as elemental composition to those of ordinary gypsum cement.

1.3 Justification of the Study

The heat treatment of phosphogypsum allows for the inertisation of impurities and also the production of anhydrite which has a wide application in the manufacturing of cement. Several treatments of methods have been considered by several authors and thermal treatment of phosphogypsum has been found to have fewer impurities than the other treatment methods (Kazragis, 2014). Furthermore, thermal treatment of phosphogypsum to temperatures over six hundred degrees centigrade results to the deterioration and expulsion of the admixtures that may obstruct the compressive strength development or create delayed setback for the setting time of the Portland cement produced (Hammas-Nasri, 2016).

Currently, complete use of phosphogypsum resource is the most ideal approach to take care of the issue of phosphogypsum waste pile contamination, and the utilization of phosphogypsum binder preparation is the principle bearing of resource reutilization. The potential to create a saleable product from phosphogypsum would be a huge economic win for the industry, creating a profit stream in place of waste management costs (Canut, 2006).

1.4 Aim and Objectives of the Study

The aim of this research work is to carry out thermal treatment of Phosphogypsum as a set retarder for Portland cement production.

This aim will be accomplished through the acknowledgment of the accompanying objectives:

1. Heating the phosphogypsum and bentonite clay mixture in a high-temperature furnace at varying temperatures and carrying out pH analysis of heated phosphogypsum.
2. Characterization of heated products by using X-ray Fluorescence (XRF), X-ray Diffraction (XRD), Scanning Electron Microscope and Energy-Dispersive X-ray Spectroscopy (SEM-EDS).
3. Determination of the gypsum purity, and production of laboratory cement with standard Portland clinker.
4. Analysis of Heat of solution of the Portland cement produced to determine the heat of hydration (HOH).

1.5 Scope of the Study

The extent of this work is restricted to thermal treatment of Phosphogypsum as a set retarder for Portland cement production and contrast with properties of normal gypsum cement.

CHAPTER TWO

2.0 LITERATURE REVIEW

2.1 Cement

Cement is a hydraulic binder material capable of setting in water or in soggy condition to create a hard mass. It is normally manufactured by finely grounding the calcined clinker produced from the combination of argillaceous and calcareous materials to produce a fine gray powder (Singh, 2019). Concrete can be followed back to the Roman articulation "creation caementicium", used to depict workmanship which is similar to modern day concrete made by utilizing crushed stone with duplicated lime as latch. The admixtures from volcanic debris and pulverized materials were added to the calcined lime, to get a hydraulic binder, were subsequently alluded to as cement (Sparavigna, 2011). Cement is rarely utilized all alone, but acts as a substance used for development which sets, hardens, and binds different materials together. It is blended with fine aggregate produces mortar for block work, or with sand and stones to produces concrete. Cement is the most extensively used material in presence and is simply behind water as the planet's generally consumed resource (Edwards, 2011). As indicated by Singh 2019, concretes used in development are by and large inorganic, oftentimes lime or calcium silicate based, and can be depicted as either pressure driven (water powered) or non-water fueled (non-pressure driven), dependent upon the limit of the cement

to set inside seeing water. Non-pressure driven (non-water powered) concrete doesn't set in wet conditions, rather it sets as it dries and reacts with carbon dioxide observable for what it's worth and it is impervious to chemical attacks by synthetic compounds in the wake of setting. Due to a complex reaction between dry matter and water, hydraulic cement (Portland cement) sets and becomes glue. The compound interactions produce mineral hydrates that are not water soluble, but are highly concentrated in water and chemically resistant. Setting in damp conditions is allowed, which protects the hardened material from chemical attack even further (Chen, 2012).

2.2 Portland Cement History

The creation of Portland cement is ascribed to Joseph Aspdin, a Leeds manufacturer and a bricklayer who got patent for it in 1824. The extravagant name of Portland was offered inferable from the similarity of this solidified cement to the trademark stone occuring at Portland in England (Medeiros and Lima, 2016).

Various sorts of Portland cement with various physical and synthetic properties are manufactured for explicit purposes. The American Society for Testing and Materials (ASTM C150) recognizes five kinds of Portland cement (Korsch and Walther, 2015).

2.2.1 Type 1 ordinary portland cement (OPC)

Ordinary Portland cement (OPC) is comprised of clinker and gypsum alone. It is the best cement due to its strength development and it is the most broadly utilized general purpose cement. It is used where cement isn't subject to run of the mill to express openings, for instance, sulphate attack from soil or water, or to a temperature rise due to warm created by hydration. Its uses incorporate asphalts and walkways, built up solid structures, spans, rail line structures, tanks, supplies, courses, sewers, water lines and workmanship work. All

Nigerian cement organizations produce this kind of cement (Korsch and Walther, 2015).

2.2.2 Type 2 (Pozzzolanic cement)

Type 2 cement are in some cases alluded to as blended cements. It is additionally universally useful Portland cement, yet it contrasts from Type 1 cement because of the way that added substances (other than gypsum) are included in its production, like limestone and pozzolan. These added substances don't adjust the quality particularly, just that a tad bit of the cement segment is diminished. It is utilized where safety measure against moderate sulfate is significant, as in waste designs, where sulfate fixations in ground waters are higher than typical, yet not extreme. It limits temperature rise when cement is set in climate since it creates less heat at slower rate than Type 1. With its moderate heat of hydration, Type 2 cements can be utilized in constructions of significant mass like projections and docks, and hefty retaining walls (Medeiros and Lima, 2016).

2.2.3 Type 3 (OPC containing higher lime to silica ratio)

This is ordinary Portland cement containing higher lime to silica ratio than Type 1 produced to achieve rapid hardening. They contain higher tri-calcium silicate, which confers higher early strength. Type 3 cements are utilized in solid works for financial benefits to accomplish fast evacuation of formwork or quick pivot of precast solid units in a shape. Streets built utilizing this kind of cement are put to utilize sooner than those developed utilizing Type1 cement (Medeiros and Lima, 2016).

2.2.4 Type 4 (OPC with low C_3S and C_3A)

These are ordinary Portland cements produced to achieve lower heat due to lower tri-calcium silicate and tri-calcium aluminate content. The tri-calcium aluminate is brought down with inclusion of iron oxide that subsequently increases tetra-calcium-alumino ferrite. These causes a lower heat of hydration that lessens heat evolution. This class of cement is planned

for mass designs like dam works when temperature rise is incredible on constant pour of concrete. In such works, if temperature is not minimized, it will cause large cracks in the structure, rendering it weak (Medeiros and Lima, 2016).

2.2.5 Type 5 (Sulphate resistant OPC)

In sulphate resistance OPC, the sulphate resistance is achieved by reducing tri-calcium aluminate (C_3A) by increasing tetra-calcium alumino ferrite (C_4AF) through iron oxide addition. These are sulphate-resisting Portland cements required in certain aggressive construction environments where high sulphate resistance is desired. Its application is appropriate where cement is to be presented to extreme sulfate assault by water or soil. Such sulfates in arrangement typically attack the hydration product of tri-calcium aluminate. Tri-calcium aluminate content, for the most part 5% or less, is required when high sulfate obstruction is required. Sulfate resistance OPC cements are of lower tri-calcium aluminate (Tsivilis *et al.*, 2000).

2.3 Cement Production Process

The raw materials needed for production of Portland cement are calcareous materials like limestone, and argillaceous material like clay and laterite at definite proportions (Korsch and Walther, 2015).

Cement production plant comprises of the accompanying cycles;

2.3.1 Quarrying crude materials

Normally occurring calcareous deposits like limestone, give calcium carbonate ($CaCO_3$) which extricated from quarries, regularly found near the cement plant. Modest quantities of "remedial" materials like iron mineral, sand is expected to give additional iron oxide (Fe_2O_3), alumina (Al_2O_3) and silica (SiO_2) to adjust the elemental makeup of the raw material mix blend to the cycle and product necessities (Harrison, 2014).

2.3.2 Size reduction/crushing

The raw material is blasted and moved to the essential crushers which breaks the materials into 10 cm enormous pieces (Harrison, 2014).

2.3.3 Pre-blending and raw meal grinding

Pre-blending involves pre-homogenization of the raw materials to keep up the necessary uniform composition of the squashed pieces in order to processed it together prior to "raw meal" grinding. Proportioning of the raw mix design by proper check and control is essential to guarantee high cement quality (Abushad and Sabri, 2017).

2.3.4 Material preheating

A preheater is a progression of vertical cyclones in which the material obtained from the raw mill is fed counter-currently with the hot gas from the rotary kiln, so the fundamental synthetic reactions happen quicker and all the more proficiently. Contingent upon the raw material dampness content, a preheater may have up to six phases of cyclones with expanding heat recuperation with every additional stage (Dunstetter *et al.*, 2006).

2.3.5 Raw material pre-calcination

Calcination is the breakdown of limestone to lime. A piece of the reaction happens in the "precalciner", a burning chamber at the lower part of the preheater over the furnace, and part in the preheater. Here, the synthetic breakdown of limestone commonly discharges 60-65% of absolute emanations. Fuel burning creates the rest, 65% of which happen in the precalciner (Dunstetter *et al.*, 2006).

2.3.6 Production of clinker in the rotary kiln

The kiln feed precalcined enters the furnace and fuel is terminated straightforwardly into the furnace to arrive at temperatures of up to 1,450 °C. As the oven pivots, around three to five times times each moment, the material slides down through continuously more sizzling zones to the burning zone. Chemical and physical reactions occur halfway that liquefy the kiln feed into clinker noodles (Dunstetter *et al.,* 2006).

2.3.7 Clinker heat recuperation and storage

The hot clinker from the kiln is conveyed onto a mesh cooler where it is cooled by approaching burning air, subsequently limiting loss of energy in the framework. A common cement plant will have clinker stockpiling betwixt clinker creation and crushing (Dunstetter *et al.,* 2006).

2.3.8 Material blending

The clinker produced is blended alongside other material admixtures. Gypsum of around 4-5% is added to control the rate of hardening of the item. On the off chance that different materials are utilized to supplant clinker such as of slag, fly debris, limestone or, the product is designated "blended cement" (Sadique and Coakley, 2016).

2.3.9 Cement milling

The clinker material is blended with gypsum and grounded into a fine grey powder, referred to as ordinary Portland cement (OPC), or grounded with mineral admixtures to make blended cement. Customarily, milling using ball mills is utilized for milling, albeit more proficient advances – vertical roller mills are utilized in numerous cutting-edge plants today (Sadique and Coakley, 2016).

2.3.10 Cement storage in the cement silo and dispatch

The final milling product is fluidized and stored in continuous flow cement silos and from which it is extracted and packed in packing station (for bagged cement) or for bulk loading in a silo truck (Sadique and Coakley, 2016). The cement manufacturing process at a glance showing the several stages is presented in Figure 2.1.

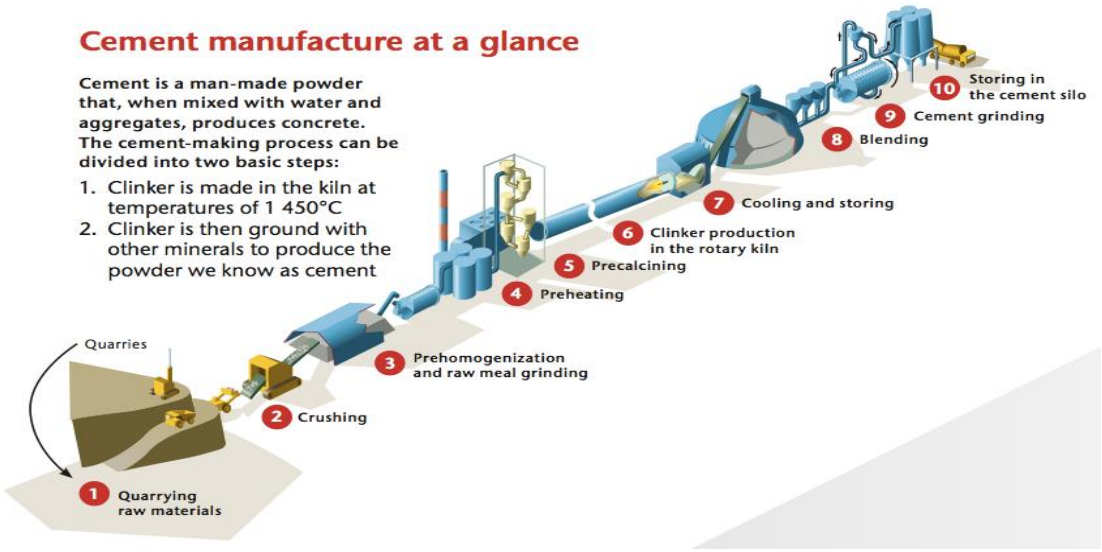

Figure 2.1: Cement manufacturing process at a glance (Sadique and Coakley, 2016).

2.4 Cement Composition

Cement is composed of major elements such as lime (calcium oxide), silica, iron, aluminum; minor elements such as potassium phosphorous, sulphur and magnesium oxide (alkali); while the trace elements are sodium oxide (Thiery *et al*., 2018).

Ordinary Portland cement consists of clinker and gypsum ground together. Clinker consists essentially of a mixture of four crystalline compounds of calcium, two have silica, one has

alumina and one has both alumina and ferric oxide. It has major constituents namely; lime, silica, alumina and ferric oxide, and minor constituents includes alkalis, magnesia and sulphur, which together amount to between 2 and 6 % by weight. In a truncated documentation, these mixtures are appointed the accompanying symbols, varying from the typical atomic notations: C_3S (tri-calcium silicate), C_2S (di-calcium silicate), C_3A (tri-calcium aluminate) and C_4AF (tetra-calcium alumino ferrite) as shown in Table 2.1. The 'C' represents lime, 'S' represents silica, 'A' represents alumina and 'F' for ferrite. Limited quantities of uncombined lime and magnesia likewise are available, alongside antacids and minor measures of different components (Thiery *et al.*, 2018).

The hydration rate is constrained by the pace of dissemination of water through the layer of calcium silicate hydrate framing on every molecule of hydrating C_3S.The most important hydraulic constituents are C_2S and C_3S. C_3S hydrates with moderate heat of hydration; hence, hydration slows down and increases as the hydrate layer thickened and this hydration reaction contributes to early strength of concrete within a week and beyond (Novotny *et al.*, 2016).

Table 2.1: Compound phase Composition of Portland cement (Novotny *et al.*, 2016)

Compound	**Chemical Formula**	**Acronym**
Tri-calcium silicate	$(CaO)_3SiO_2$	C_3S
Di-calcium silicate	$(CaO)_2SiO_2$	C_2S
Tri-calcium aluminate	$CaO_3(Al_2O_3)$	C_3A
Tetra-calcium alumino ferrite	$CaO_4Al_2O_3Fe_2O_3$	C_4AF

Tri-calcium silicate (C_2S) hydrates all the more gradually and offers more to late strength of concrete at 28 days and past related to lingering unhydrated C_3S. Tri-calcium aluminate (C_3A) hydrates quickly and savagely and is answerable for speedy setting yet contributes

little to strength. This clarifies the speedy setting of high alumina cements like the early Roman cements. Tri-calcium aluminate (C_3A) and tetra-calcium alumino ferrite (C_4AF) contribute little to strength and construction of cements (Novotny *et al.*, 2016). The clinker phases comprising of the cement constituents can be theoretically gotten using Bogue's Equation according to Equations (2.1-2.6).

$$C_3S = 4.070\ CaO_1 - 7.6\ SiO_{2\,sol} - 6.72\ Al_2O_3 - 1.43\ Fe_2O_3 \quad (2.1)$$

$$C_2S = 8.60\ SiO_{2\,sol} + 5.07\ Al_2O_3 + 1.08\ Fe_2O_3 - 3.07\ CaO_1 \quad (2.2)$$

$$C_3A = 2.650\ Al_2O_3 - 1.69\ Fe_2O_3 \quad (2.3)$$

$$C_4AF = 3.040\ Fe_2O_3 \quad (2.4)$$

$$CaO_1 = \text{associated lime} = CaO_{total} - CaO_{free} - 1.270\ CO_2 - 0.70\ SO_3 \quad (2.5)$$

$$\text{and} \quad SiO_{2\,sol} = \text{soluble silica} = SiO_{2\,total} - SiO_{2\,insoluble} \quad (2.6)$$

2.4.1 Mechanical performance of different cement phases

Chemical reactions that happen when clinker is produced are mind boggling inferable from the way that the majority of the reactions happen in a rotational kiln, which makes it hard to notice straightforwardly. Cement clinker and lime consists of oxides of silicon (Si), calcium (Ca), alumina (Al), and iron (Fe) (Thiery *et al.*, 2018). The reaction between clinker and lime is an exothermic reaction in which lime reacts with the acidic oxides to give the mineral compounds which are C_3S, C_2S, C_3A, and C_4AF as shown in Table 2.2.

Table 2.2: Exothermic reactions in clinker and lime formation**(**Chaunsali and Peethamparan, 2011).

Chemical Reactions	**Temperatures needed for reactions to occur (^{0}C)**	**Enthalpy changes (25^0C) ΔH(kJ/kg reactant)**
$C + 0_2 \rightarrow C0_2\,(g)$		-32803
$2CaO + Si0_2 \rightarrow Ca_2Si0_4\,\beta\,C(g)$	600 - 1300	-734
$3CaO + SiO_2 \rightarrow Ca_3Si0_5$	1330 - 1450	-495
$3CaO + \alpha\text{-}Al_2O_3 \rightarrow Ca_3Al_20_6$		-27
$6CaO + 2\alpha\text{-}Al_2O_3 + \alpha\text{-}Fe_2O_3 \rightarrow Ca_6Al_2\,O_{12}Fe_2$		-157

$4CaO + \alpha\text{-}Al_2O_3 + \alpha\text{-}Fe_2O_3 \rightarrow Ca_4Al_2O_{10}Fe_2$		-105
Formation of C_2F and C_3A	800 - 1250	-

This cement constituents can be compared with the compressive strengths as shown in Figure 2.2. The C_3S and C_2S are responsible for the early and later strengths while C_3A is responsible for its plasticity and C_4AF is gives the gray colouration in cement products. The compressive strengths increase with increasing temperature

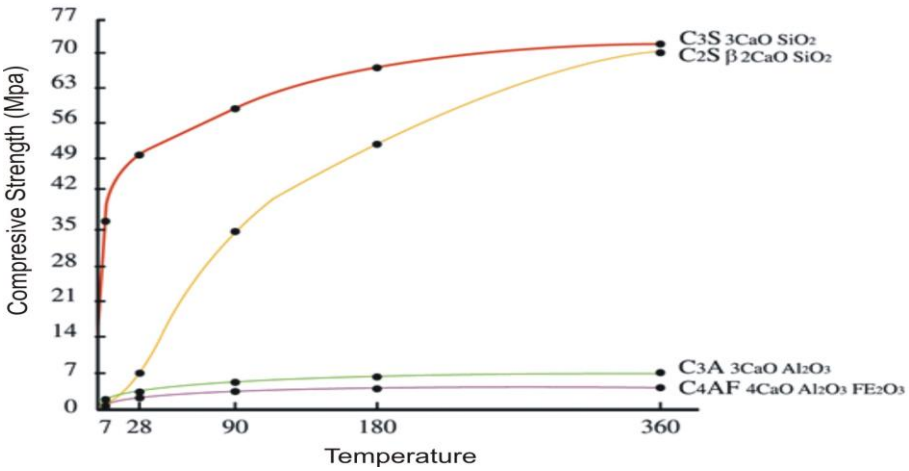

Figure 2.2: Comparison of compressive strengths of cement constituents (Dunstetter *et al.*, 2006).

2.4.2 Cement clinker phase chemistry

Some reactions that occur during the production of cement clinker and lime are presented in Equation 2.7-2.9. When heating the materials, the dominant reactions are the calcinations of

limestone and formation of alite (C_3S) and belite (C_2S) as shown in Figure 2.3 (Ali *et a*l., 2017).

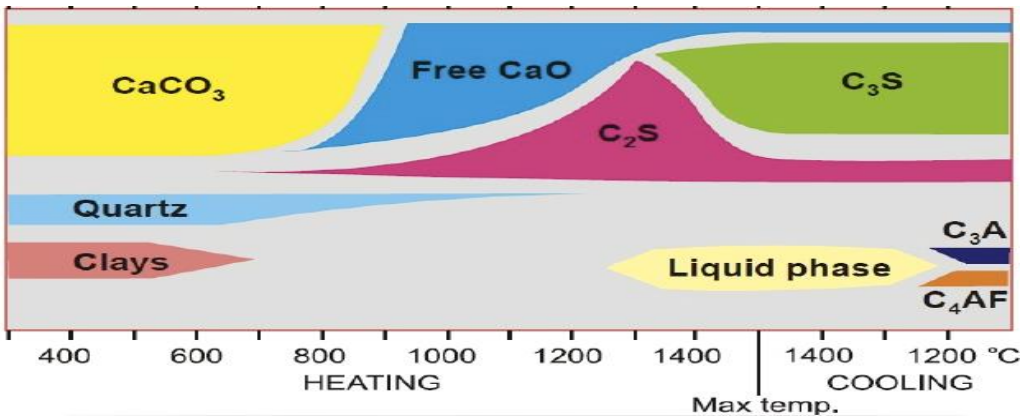

Figure 2.3: Schematic diagram of clinker formation reactions (Punmatharith *et al.*, 2010)

The lime reacts with the decomposition of clay products which eventually forms C_3A and C_4AF. A liquid (oxide melt) is formed at 1300 ^{0}C that promotes the formation of C_3S (Punmatharith *et al*., 2010). The main mineral liquid phases formed in the clinker are observed using an optical microscope as presented in Figure 2.4.

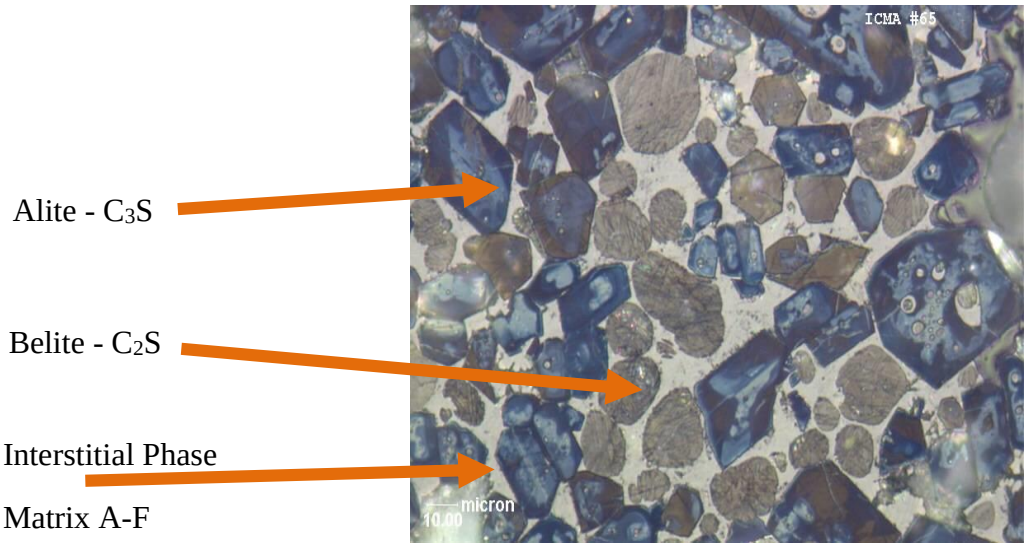

Figure 2.4: Optical Microscope of the Cement Constituents. (Bennis *et al.,* 2010)

The connection between the four fundamental oxides is depicted in cement production by the lime immersion factor (LSF), silica modulus (SM), and alumina modulus (AM), which are determined from the crude material syntheses (Suárez *et al*., 2016). Equations (2.7-2.9) gives the proportions which decide the fundamental properties of cement and certain process qualities.

$$LSF = \frac{CaO}{(2.8\times SiO_2 + 1.18\times Al_2O_3 + 0.65\times Fe_2O_3)} \times 100\% \quad (2.7)$$

$$SM = \frac{SiO_2}{(Al_2O_3 + Fe_2O_3)} \quad (2.8)$$

$$AM = \frac{Al_2O_3}{Fe_2O_3} \quad (2.9)$$

2.5 Cement Testing

i. Physical testing: This includes liter weight test, fineness test, normal consistency test, loss on ignition, compressive strength test, soundness test and calcination test.

ii. Chemical Testing: This includes free lime test, test of elemental compositions of cement (NIS, 444- 2003).

2.5.1 Fineness test

The test for fineness in cement is utilized to decide the how porous or permeable a cement product is. It has a significant job in the concrete creation by improving the effectiveness of

the comminution (decrease of strong materials) measure. Better concrete offers a more noteworthy surface region for hydration (Liaqat and Saeed, 2011).

Cement fineness can be tested either by the sieve method or by the Blaine method.

(i) By sieve method

The cement sample is agitated on a mesh sieve that is subjected to either vibratory sieving (vertical movement) or horizontal sieving (horizontal motion) after which the particles (residue retained) are compared with the apertures of every single sieve as shown in Plate 2.1. During this process, a precautionary measure taken during this cycle is to ensure that prior to sieving, air set chunks of concrete ought to be broken. Additionally, the sieving ought to be finished by pivoting the strainer and not by interpretation (Liaqat and Saeed, 2011).

The manufacture of cement particles in which the grain size is bigger than the predefined sieve size is given by Equation (2.10).

$$F = \frac{R_0}{C} \times 100\% \qquad (2.10)$$

Where R_0 = mass of residue in grams

C = mass of cement measured (10g)

F = Correction factor (Percentage residue)



Plate 2.1: Mesh sieve method of cement's fineness

(ii) By Blaine method

Determination of fineness utilizing the Blaine technique is done using a Blaine device as shown in Plate 2.2 by sucking in a definite amount of air through a prepared bed of cement of distinct porousness. The fineness is communicated as absolute surface region in square centimeters per gram (Chang, 2004). Cement quantity of 2.95g is estimated and put in the punctured circle at the edge of the lower part of the cell on another filter paper to give the cement bed porosity. Pour the quantity of cement weighed in the cell avoiding any loss of the weighted cement. Touch the surface of the cell to even out the cement and affix the new ash less filter paper on the levelled-out cement and pack the cement with the plunger until the plunger cap is in contact with the top of the cell. Gradually pull out the plunger at a brief distance pivoted at 90^0, subdue the cement bed, and afterward gradually pull out completely. Join the porous cell to the manometer tube with a sealed shut association and gradually clear the air in the manometer U-tube until the fluid arrives at the top imprint, at that point firmly close the worth. Start the clock when the lower part of the meniscus comes to close the apex

imprint and stop as soon as the lower part of the meniscus arrives at the base imprint. Record the time it takes utilizing stopwatch. The Blaine apparatus constantly varies from one apparatus to the next relying upon the thickness of the adjustment of the device and the density of the cement sample to be tried with the Blaine device (Chang, 2004). The surface area is gotten using Equation (2.11).

$$S_s = \sqrt{t} * k \qquad (cm^2/g) \qquad (2.11)$$

Where S_s = Specific surface area

k = Apparatus constant (540)

t = time



Plate 2.2: Blaine apparatus

2.5.2 Standard consistency of cement paste

Consistency of cement paste helps to obtain the workability of the sample of cement in order to know the ratio of water to cement ratio that will be needed to make cement paste workable. For the most part, the normal consistency of cement paste varies from 26-33%. The test assists with deciding moisture content for different analysis like setting time, expansion of a cement, and compressive strength (Tsivilis *et al*., 2000).

The water-cement ratio in percentage needed to make cement paste of standardized consistency is given in Equation (2.12);

$$N = \frac{W}{M} \times 100\ \% \qquad (2.12)$$

Where; N= Normal consistency, W = amount of water required and M = amount of cement to be utilized

Cement quantity of 500g and 140 mL distilled water is measured and put in the mixer for mixing. The time taken during the process where the cement paste is blended called the 'gauging time' is recorded and this ought not be in excess of 5 min. Fill the circular Vicat form, settling on a metal plate with this cement paste, making it level with top of the shape by smoothing the excess paste ensuing the shape is levelled completely. Place it under the pole bearing plunger, bring down the plunger tenderly in order to contact the rare end of the plunger and rapidly discharge the plunger so that it presses against the ash less paper on to the paste as seen in Plate 2.3. Measure the depth of infiltration of the plunger which should

be between 5-7 mm. Then place the mould into the humidity cabinet at a temperature of 20 ^{o}C (EN 196-6 2005).



Plate 2.3: Vicat apparatus for Consistency of standard cement paste

2.5.3 Cement paste setting time test

The period at which a cement paste set is affected by water to cement ratio, cement fineness, and sulphite content of gypsum. Setting time tests helps to evaluate how cement paste sets. Typically, the setting time test are of two folds: initial set which occurs when the paste is beginning to gain plasticity significantly and final set occurs when the cement has gained plasticity and solidified at which it can support some load (Naik *et al*., 2001). For control purposes, the initial setting time is not sooner than 75 min as contained in NIS 444:2003 and not later than 160 min. Additionally, setting time indicates if a cement paste hydrates normally or not.

These specific periods are discretionary focuses used to portray cement; they don't have any essential substance importance. There are two basic setting time tests: Gillmore needle test

and Vicat needle test. The setting time test using the Vicat needle is generally normal and will result to limited times compared to the Gillmore needle test (ASTM C191-19, 2019).

Setting time of cement is of two stages:

1. **Initial setting time (IST):** The period between the moment that the water is mixed with the cement, to the period that the paste starts losing its versatility/plasticity is referred to as initial setting time. It is the period between the moment water is added to the cement and the period at which 1 mm^2 area needle infiltrate the cement paste place in the Vicat mould going from 5-7 mm from the lower part of the mould as shown in Plate 2.4.
2. **Final setting time (FST):** The period elapsed between the moments at which water and cement are mixed, to the period when the paste has totally lost its pliancy (plasticity) and has achieved adequate immovability to oppose certain pressure is referred to as the final setting time (Chang, 2004).

In genuine development managing cement paste, mortar or solid; setting time is needed for blending, moving, putting, compacting and wrapping up. During this time cement paste, mortar, or concrete ought to be in plastic condition (ASTM International, 2008a). The setting time is obtained using equations (2.13) and (2.14).

$$\text{Initial setting time} = t_2 - t_1 \quad (2.13)$$

$$\text{Final setting time} = t_3 - t_1 \quad (2.14)$$

Where; t_1 = period at which water and cement is first added together (gauging time)

t_2 = period at which when needle penetration falls between 3-5mm from the mould's bottom

t_3 = period at which an impression is made but attachment fails to do so.

The following safety precautions should be ensured while carrying out the compressive test analysis: (i) Clean the Vicat needles each time it is utilized and the situation of the shape ought to be moved marginally after every entrance to keep away from infiltration at a similar spot for the underlying and last setting time. (ii) The Vicat needles ought to be delivered tenderly every time it is utilized in deciding the underlying and last setting time.

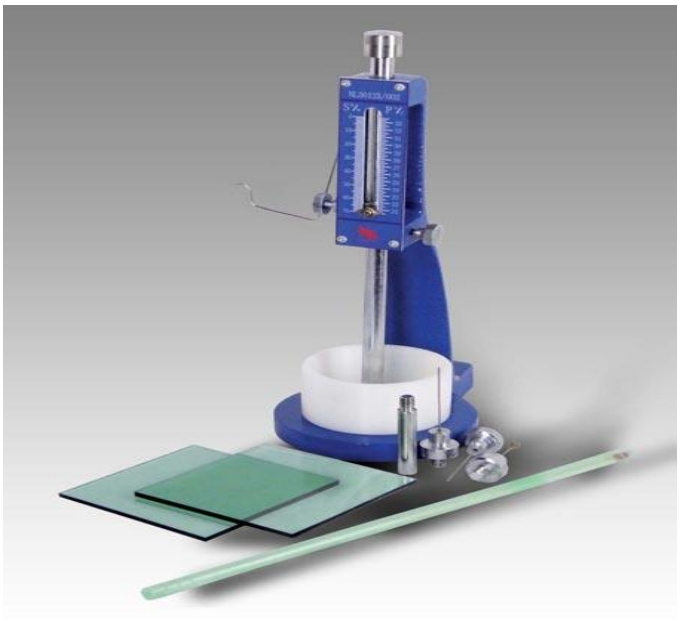

Plate 2.4: Vicat Apparatus for setting time test

2.5.4 Cement compressive strength test

Cement compressive strength is one of the vital of the relative multitude of quality parameters. Compressive strength is the limit of a material or construction to withstand loads. It tends to be estimated by applying power on it utilizing compressive machine. Accordingly, it isn't astonishing that cement is constantly tried for its mechanical strength at the laboratory before the concrete is utilized for significant works by making moulds using the compressive mould as presented in Plate 2.5. Strength tests are not made on concrete paste due to over-the-top shrinkage and ensuing cracking of cement. Strength of cement is indirectly found on

cement, water and sand in explicit extents. The standard sand is utilized for discovering the strength of cement while compressing it using a compressive machine as shown in Plate 2.6. Since concrete increases strength over the long haul, the compressive strength period is determined essentially to be 2, 7 and 28 days (ASTM C 109, 2016).

Compressive strength (S): $S = \frac{F}{A}$ (2.15)

Where; F = Force, A = Area

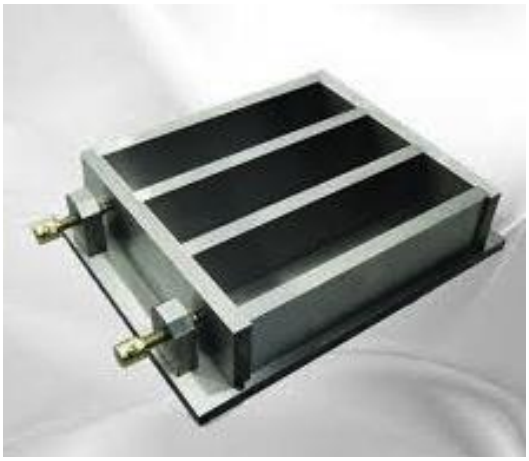

Plate 2.5: Compressive strength gang/mould

The following Precautions should be ensured while carrying out the compressive test analysis: (i) The cubes should be tested; also, the moulds should be placed sideways and not on their faces. (ii) The moulds compressive strength ought to be determined as soon as it is taken out of the curing tank and not permitted to dry.



Plate 2.6: Compacting machine

2.5.5 Loss on ignition of cement

The ignition loss of cement sample is dictated by heating it up to a temperature of around 1000 ^{0}C until a steady weight is acquired, which is lower than the underlying weight before start after which the loss in weight of the sample because of heating can then be decided. The weight loss because of loss on ignition on start demonstrates the presence of unstable substances like CO_2, which might be brought about by fragmented deterioration and delayed stockpiling or adulteration during transportation (Heiri *et al.,* 2001). In the cement industry, the worth of Loss on ignition on start of the cement or its blend is generally identical to the

loss in mass that will go through heat treatment. The standard Loss on ignition test is contained in (NIS 445;2003).

2.5.6 Specific gravity

The extent of the weight of a volume of the substance to the greatness of an identical volume of the datum reference substance. It is ordinarily utilized in combination proportioning estimations. Specific gravity of any material is normally determined using water, because water is the best material to use. However, when water is added to cement, a compound is formed (carbon oxide), while kerosene and cement do not react together. Ordinary Portland cement specific gravity is by and large around 3.15 (Mamouk and Zaniewski, 2011).

2.5.7 Hydration enthalpy (HOH)

The hydration enthalpy also referred to as the heat of hydration of cementitious materials by and large is exothermic, demonstrating a variety in the freed heat which reflects the hydration system of the hydrating material. The calorimeter apparatus is used in determining the HOH as seen in Plate 2.7. The compounds of Portland cement which includes; alite (C_3S), belite (C_2S), tricalcium aluminate (C_3A) and tetra-calcium alumino ferrite (C_4AF) reacts with moisture to form hydrates which lead to the setting and solidifying of the cement. It is accepted that the reactions of each compound occur independently (Abla, 2013)

The main reactions of the individual cement compound are as follows;

1. During the hydration process of cement, alite (C_3S) and belite (C_2S) react with moisture to produce calcium hydroxide $Ca(OH)_2$ and calcium silicate hydrate (CSH).
2. The tricalcium aluminate (C_3A) not only reacts with water directly, but also reacts with $CaSO_4.2H_2O$ (gypsum) to produce cement bacillus (ettringite). When all the gypsum is spent, the ettringite gets flimsy and reacts with unreacted C_3A to form monosulphate aluminate hydrate crystals.

3. Tetra-calcium alumino ferrite (C_4AF) reacts with gypsum water to form ettringite, lime and alumina hydroxides. The complete product is attained by further reaction of C_4AF with ettringite. The main reactions of the individual cement compound are accompanied by heat liberation. The liberated heat of hydration is one method to determine extent of hydration (Abla, 2013).



Plate 2.7: Calorimeter apparatus for HOH

The heat of hydration is a significant boundary in cementitious materials wherein reactions discharge a lot of heat (Abla, 2013). This delivery may cause the arrangement of breaks and an adjustment of temperature, which weaken the sturdiness and effectiveness of the mortars (Abushad and Sabri, 2017). According to Baran and Pichniarczyk, (2017), a decrease in hydration heat is gainful to the mortar by diminishing the straight shrinkage, which may cause surface breaks and microstructural distinguishes. Be that as it may, inordinate heat decrease could weaken the mechanical strength for generally more elevated levels of waste joining (EN 196 -8:2003).

The hydration enthalpy as a function of the time can be categorized with specific characteristics into the following stages; (i) pre-induction; (ii) induction; (iii) acceleration; (iv) post-acceleration and (v) diffusion-limited reaction as seen in Figure 2.5.

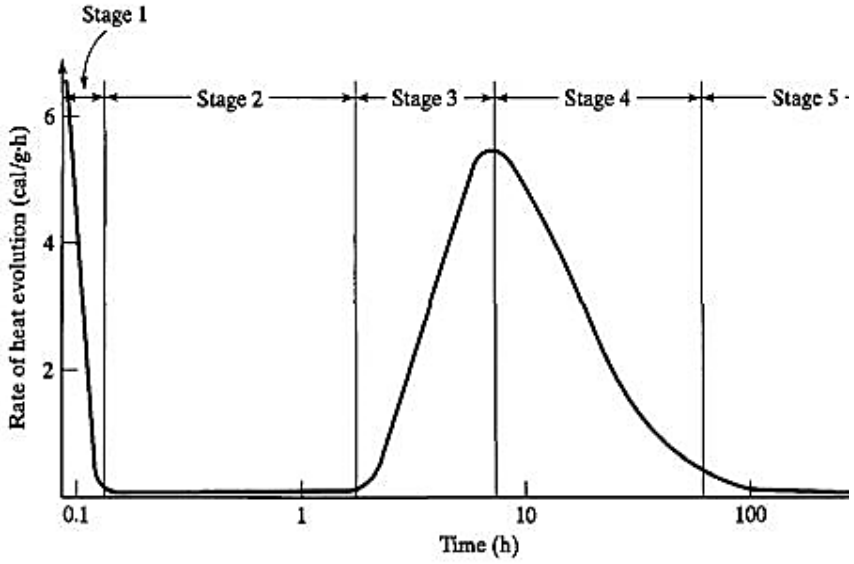

Figure 2.5: Heat development rate during hydration of tri-calcium silicate (Abla, 2003)

The hydration enthalpy released is highest during the acceleration and the post-acceleration phase, which ordinarily occur between two and ten hours from the beginning. Curing concrete temperature and strength development is fundamental to in-service concrete performance. Undesirable temperature development may cause concrete to crack under some natural conditions, and it may bring about inadequate strength advancement (Chang, 2004).

Heat of hydration is created by the reactions of aluminate (C_3A) and belite (C_3S) in cement. The heat of hydration is likewise affected by water to cement proportion, fineness and restoring temperature. Increase in any of the elements builds heat of hydration (Chang, 2004). This is the case normally observed of huge mass solid constructions such as gravity dams.

The pace of heat delivered is altogether quicker than it tends to be dispersed. This in turn makes high temperatures in the focal point in the huge solid masses that thus may make unwanted stresses as the solid cools to surrounding temperature. The benefit of high heat of hydration is appreciated in winter in light of the fact that good relieving temperatures are looked after (Chang, 2004).

According to EN 196 -8:2003, hydration enthalpy for cement with heat that are low is confined to an extent of 270.0 kJ/kg, while for cements with heat that are very low, the most extreme is 220.0 kJ/kg. A requirement of an extent of 290 kJ/kg is for type 2 cements with optimal hydration enthalpy and an extent of 250.0 kJ/kg for type 4 cement with hydration enthalpy that are very low (Ayres *et al.,* 2001). The estimation of the hydration enthalpy of Portland cements making use of the heat of solution has become in vogue as the acceptable standards nationally. The method of estimating the heat of solution in every seven days during a specific time of hydration betwixt the hydrated and unhydrated heat of dissolution can be obtained by combineing nitric and hydrofluoric acid.

2.6 Phosphogypsum

Phosphogypsum (PG) is a concomitant from superphosphate fertilizer company by the interaction of tetraoxosulphate (vi) acid on phosphate rock, and is commonly used as a beneficial fertilizer for soil treatment. During the wet interaction process illustrated in Figure 2.6, about 4-5 tons of PG is created when 1 ton of phosphate rock is attacked with sulphuric acid, and this waste pile is either stacked in open piles or washed out into water courses (Al-Hwaiti *et al*., 2010). The reaction between phosphate rock and tetraoxosulphate (vi) acid

produces phosphoric acid in accordance to reaction given in Equation (2.16), where X could be hydroxide, fluorine, chlorine, or bromine (Ayres *et al*., 2001).

$$Ca_5(PO_4)_3X + 5H_2SO_4 + 2H_2O \rightarrow 3H_3PO_4 + 5CaSO_4.2H_2O + HX \qquad (2.16)$$

Phosphogypsum comprises of calcium sulphate dihydrate ($CaSO_4.2H_2O$) and some various impurities which encompasses phosphoric oxide, fluorine and some natural matter, which seriously impedes the industrial use of phosphogypsum directly in cement industry as a retarder. The annual phosphogypsum production is projected to extend, especially within the Nigerian Southwest, since Dangote Industries Limited is building one among the most important fertilizer industries (Okeowo, 2016). Phosphogypsum are land filled into the environmental and this results to contamination as a result of the inappropriate waste disposal, or a lack of understanding and monitoring of this activity. This may have an impact on ecosystem functionality, sustainability, and biodiversity, resulting in irreversible damage to chemical, physical, and biological aspects as seen in Figure 2.7. (Rashad, 2017).

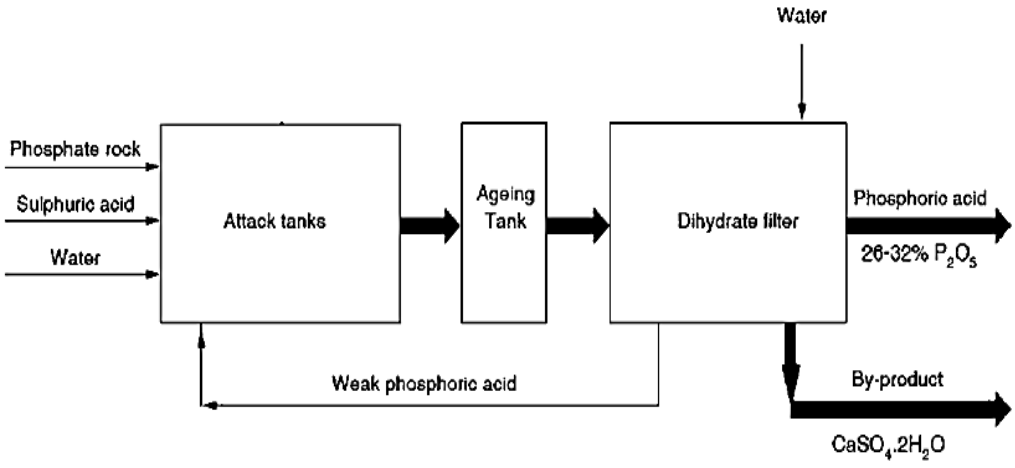

Figure 2.6: Wet Process of Phosphoric Acid Production (Degimency, 2008)



Figure 2.7: Phosphogypsum landfill of about 30m depths (Degimency, 2008)

Expanding use is being made of removal in ordinary landfill facilities set up for industrial or perilous waste; some of the time with some extra radiation insurance measures being applied. Acknowledgment measures for landfill removal, communicated regarding greatest radionuclide movement focus, have been set up in a few nations, with values going from 5 to 10 Becquerel/gram (Bq/g) (Oumnih *et al.*, 2017).

The objective for phosphogypsum is pressing, since the world rural interest is expanding and it is liable for the rise of this natural issue. There are a few prospects of utilization of this material, like common development, remembering cost decrease for lodging development, clearing roads, farming as therapeutic physical and compound attributes of soil, in wastewater treatment (Degimency, 2008).

Considering the qualities of phosphogypsum and its appealing monetary potential right now using phosphogypsum as an alternative crude material for various applications has sparked a lot of curiosity. Supplanting of clinker noodles alongside certain amount of phosphogypsum could be of great value in concrete and cement despite the fact that there is still discussion in related literary works (Canut, 2006). The impact of phosphogypsum expansion with cement clinker on the characteristics of paste, mortar, and concrete is the focus of this study. The

effect of phosphorus in phosphate rocks has been examined in order to authenticate the utilization of quarries containing phosphorus-rich limestone since 1950 (Belboom, 2015). Ordinary Portland cement usually consist of phosphorus in the range 0.2-0.3 weight percent phosphoric oxide (P_2O_5) (Kwon *et al.,* 2005). The major ionizing radiation source in the coastal area of Dakar in Senegal was potassium (^{40}K), uranium (^{238}U) and thorium (^{232}Th). The ionizing radiation source of ^{40}K was (260.57±31.17 $Bq.kg^{-1}$) with a maximum value of 616 $Bq.kg^{-1}$, while ^{238}U and ^{232}Th results of activity concentration were relatively low with an average value of 17.04±2.21 $Bq.kg^{-1}$ and 12.82±0.75 $Bq.kg^{-1}$ respectively. In term of radiological assessment, the radium equivalent activity measured in the sample was below the recommended limits, as well as external hazard index (Djicknack *et al.,* 2018)

Thermal treatment of phosphogypsum decontaminates the impurities present in it, because phosphogypsum binding characteristics are impeded by the presence of hydrogen fluoride, phosphoric acid (H_3PO_4) and calcium hydrogen phosphate dihydrate $Ca(H_2PO_4)_2.2H_2O$. When phosphogypsum is heated to temperatures above 100 ^0C, hydrogen fluoride dissolves in the moisture and evaporates. Phosphoric acid on the other hand transforms into pyrophosphorous (diphosphoric) acid when heated according to Equation (2.17).

$$2H_3PO_4(> 215\ °C) \rightarrow H_4P_2O_7 + H_2O \qquad (2.17)$$

During heating of the compound, diphosphoric acid later polymerisizes into polymetaphosphoric acid according to the reaction in Equations (18) and (19) respectively. Heating phosphoric acid present in phosphogypsum waste to temperatures greater three hundred degrees centigrade completely decomposes it, and it is being evolved as phosphorous oxide (P_2O5) and water (H_2O).

$$n\ H_4P_2O_7\ (> 300\ °C) \rightarrow 2(HPO_3)n + n\ H_2O \qquad (2.18)$$

Where, (n = 3-8):

$$2(HPO_3)n \rightarrow nP_2O_5 + n\,H_2O \quad (2.19)$$

Calcium dihydrophosphate present in phosphogypsum is decomposed as shown in Equations (2.20) and (2.21) respectively. The Calcium dihydrophosphate completely decomposes and P_2O5 and H_2O are evolved.

$$Ca(H_2PO_4)_2 \cdot H_2O\ (100 - 110\ °C) \rightarrow Ca(H_2PO_4)_2 + H_2O \quad (2.20)$$

$$2Ca(H_2PO_4)2\ (150 - 200\ °C) \rightarrow Ca_2P_2O_7 + P_2O_5 + 4H_2O \quad (2.21)$$

2.6.1 Previous work carried out on phosphogypsum

Erdogan *et al*., (1994) explored the impact of washing phosphogypsum with water and slake lime, with the inclusion of heat treatment before and after the process. The two of them revealed that the untreated phosphogypsum impeded the setting time of Portland cement and furthermore decreased its strength, yet it may be utilized in controlling the hydration of cement whenever washed with slake lime [$Ca(OH)_2$].

Singh, (2002) adopted a technique that comprises of wet sieving the example, and the outcomes have shown that the pollutants were terribly decreased in the better portions. Using a 100-m sifter, Al-Jabbari et al. (1988) rinsed the phosphogypsum with water. Afterwards, the phosphogypsum was heated and gas pedals added (for instance, calcium hydroxide) to the sintered item to enhance the setting time and compressive strength of the material produced.

Jaroiski *et al*., (1993) portrayed a technique in which he initially filtered the phosphogypsum in a 12% (mass proportion, m/m) sulphuric corrosive answer for recuperate uncommon earth components, trailed by transformation into the 6-anhydrite type of calcium sulfate in a half 50% (m/m) sulphuric acid arrangement. This strategy was effective in eliminating the bothersome debasements like mixtures of phosphorus, fluorine and sodium. The chemical components of imported phosphate stone on a regular basis from different countries and the

level of contaminants is presented in Table 2.3

Table 2.3: Chemical components of imported phosphate stone (Fertilizer Association of India, Central Pollution Control Board, 2014)

Country/ Constituents	**Morroco**	**Senegal**	**Togo**	**Egypt**	**Australia**	**Syria**	**Tunisia**
P_2O_5	32.85	36.40	35.25-36.16	28.0-28.8	31.45	28.01-28.90	33.90
CaO	50.84	50.15	50.5	46.0-47.9	50.15	47.9-50.0	51.00
SiO_2	1.93	3.00	5.0-7.0	6.21-7.13	2.80	5.01-8.00	2.00
F	4.00	3.50	3.9-4.1	3.20-3.61	3.73	2.01-3.51	-
MgO	0.29	-	0.30	0.32-0.51	0.80	0.41-1.21	0.19
Organic compounds	0.29	0.13	0.04	0.07-0.30	-	0.40-0.61	-
Cl (ppm)	100-200	120	400	-	300	-	-
CO_2 as $CaCO_3$	4.94	-	1.65	3.4-5.8	6.00	5.01-8.01	-
K_2O	0.69	0.01	0.02-0.06	-	0.11	-	-

Country/ Contituents	**Vietnam HG**	**China**	**Florida**	**African Pharla-Bowar**	**Brazil**	**Russia**	
						Kola	Kodar
P_2O_5	33.19	35.10-36.25	34.2	36.8	34.50	38.8	37.01
CaO	32.30	49.40-50.62	49.9	52.1	50.40	50.5	52.5
SiO_2	12.0	3.63-3.88	3.6	2.6	3.46	1.11	2.03
F	2.50	3.41-3.50	3.8	2.2	3.70	3.31	0.82
MgO	2.0	-0.69-1.12	0.2	1.1	1.65	0.11	2.10
Organic compounds	-	0.37-0.46	0.2	0.1	0.32	0.10	0.20
Cl (ppm)	-	-	-	-	-	-	-
CO_2 as $CaCO_3$	0.8	1.97-2.52	3.1	3.5	4.21	0.20	-
K_2O	-	0.10-0.20	0.11	0.11	-	0.51	-

2.7 Clay

The main component of clays is formed from hydrous aluminum silicates brought about by the weathering of alkali and alkali earth containing aluminum silicates and their chemical conversion products, feldspar and mica. Based on these, clays are grouped as kaolin, montmorillonite, and alkali bearing clays (Zakaraya *et al.*, 2009). Clay has an assortment of actual qualities like versatility, shrinkage enduring an onslaught and under air-drying, grain fineness. Muds are hydrous alumino-silicates, which made out of combinations of fine-grained mud minerals, precious stones of different minerals, and metal oxides. The components of clay groups are shown in the Table 2.4.

Table 2.4: Components of clay samples (Won *et al.*, 2012)

Clay groups	Clay Minerals	Components
Kaolin	Kaolinite	$Al_2O_3.2SiO_2.2H_2O$
	Dickite	$Al_2O_3.2SiO_2.2H_2O$
	Nacrite	$Al_2O_3.2SiO_2.2H_2O$
	Halloysite	$Al_2O_3.2SiO_2.2H_2O$
Montmorillonite	Montmorillonite	$Al_2O_3.4SiO_2.nH_2O$
	Beidellite	$Al_2O_3.3SiO_2.nH_2O$
	Nontronite	$(Al,Fe)_2O_3.3SiO_2.nH_2O$
Alkali Clays	Illite	$K_2O.MgO.Al_2O_3.SiO_2.H_2O$

Clay varies chemically from those close to pure clay to those containing iron hydroxide, iron sulphide, and calcium carbonate. The principal colouring agent in clays is iron hydroxide,

clays with no impurities is white but organic matter in clay may also give it different colours (Felhi *etal.,* 2008).

2.7.1 Types of clay

2.7.1.1 *Montmorillonite*

Montmorillonite is an extremely delicate phyllosilicate mineral that normally shapes in infinitesimal precious stones, framing clay. Montmorillonite, a member of the smectite family has a 2:1 gem grid extension and belong to a group of non-metallic clays mostly composed of hydrated sodium calcium aluminum silicate, as well as a collection of monoclinic mud minerals as shown in Figure 2.8 (Reeves *et al.*,2006).

The essential primary structure is a layer comprising of two internal pointing tetrahedral sheets with a focal alumina octahedral sheet. In the length and breadth headings, the layers are uniform, but the connections between them are fragile and have amazing cleavage, allowing water and other particles to penetrate between the layers, producing development in the height bearing area. Isomorphs substitution causes a net lasting charge adjusted by cations in such a way that water can pass between the sheets of the precious stone cross section, resulting in a reversible cation-trade and plastic characteristics. (Kautz and Ryan, 2003).

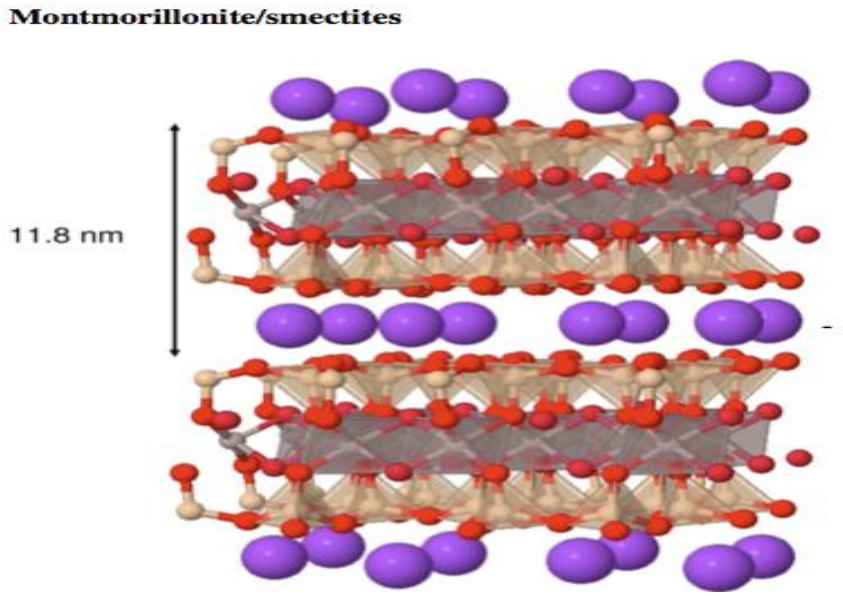

Figure 2.8: Montmorillonite (Kautz and Ryan, 2003)

2.7.1.2 ***Metabentonite***

Bentonite is typically shaped from enduring of volcanic debris, frequently within the sight of water. In any case, the term bentonites, just as comparative clay called tonstein, have superb rheological and spongy properties for modern purposes. Minerals from clay is the enduring result of mafic silicates, and is steady in parched, semi-bone-dry, or calm environments. It can adsorb a lot of water, shaping a watertight boundary. It is utilized widely in the oil boring industry, common and ecological designing and the substance business where it is known as bentonite (Won., *et al*, 2012).

Bentonite clay has remarkable colloidal qualities, and it is frequently used in drilling mud for oil and gas wells, as well as for geotechnical and environmental investigations. There are two types of bentonite: sodium bentonite and calcium bentonite. When wet, sodium bentonite expands, absorbing up to a few times its dry mass in water (Won., *et al*, 2012). Bentonite clay minerals have little molecule size and complex permeable design with high explicit surface territory, which permits solid physical, compound associations with broke up species.

2.7.1.3 *Kaolinite*

According to Kautz and Ryan (2003), the kaolinite bunch incorporates the dioctahedral minerals kaolinite, with an Equation of $Al_2Si_2O_5(OH)_4$ alongside a 1:1-layer structure, with one of its plane faces comprises of silica tetrahedral and the other of alumina octahedral as shown in Figure 2.10. The design of all around solidified kaolinite is uncharged and the exchange capacity is immaterial. Kaolin is a delicate, white plastic clay comprising fundamentally of the mineral kaolinite which is a hydrated aluminum silicate $Al_2Si_2O_5(OH)_4$ (Murray, 2002).

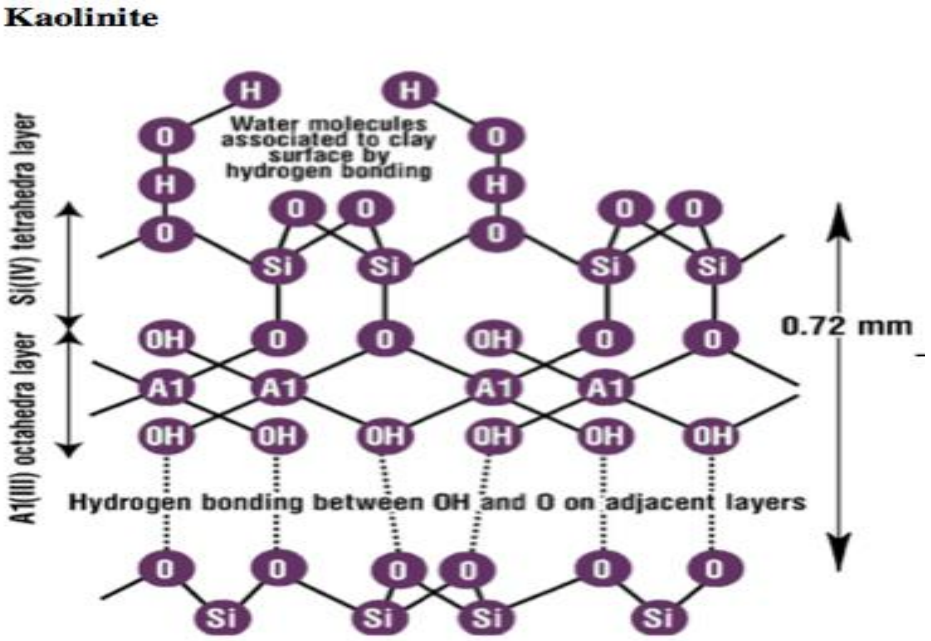

Figure 2.9: Kaolinite (Murray, 2002)

Heat treatment in air at an environmental pressuring factor causes the kaolinite bunch clay to go through a series of stage alterations. Dehydroxylation with an endothermic reaction parchedness starts at 550-600 °C to create scattered meta-kaolin, $Al_2Si_2O_7$, yet nonstop hydroxyl misfortune is seen up to 900 °C and this is credited to steady oxolation of the metakaolin. The fact that kaolinite contains a heterogeneous surface charge is important

because the basal surface of kaolinites is thought to transmit a consistent primary charge, which is attributed to isomorphous replacement of Si^{4+} by Al^{3+} (Gupta *et al*., 2011).

CHAPTER THREE

3.0 MATERIALS AND METHODS

3.1 Materials

The materials and equipment used in the course of carrying out this research work are as follows: the clinker samples were collected from Obajana cement plant Obajana Kogi State, which is one of the foremost indigenous cement companies in Nigeria. The limestone and bentonite clay were obtained from Iwa/Oyo in Kogi State and the Phosphogypsum was obtained from Dakar, Senegal. The phosphogypsum sample as well as the parent clinker sample is presented in plate 3.1, while the heated phosphogypsum-clay mixture and bentonite clay sample is presented in Plate 3.2.



(a) (b)

Plate 3.1: Sample of (a) Phosphogypsum (b) Clinker



(a) (b)

Plate 3.2: Sample of (a) Heated PG and Clay mixture (b) Bentonite Clay

The equipment specification, model and manufacture used in carrying this research work is presented in Table 3.1.

Equipment/Apparatus	Specification	Model	Manufacture

XRF/XRD Analyzer	ARL 9900 Series Maximum output 60 kV (70 kV optional), maximum current is 120 mA	ARL 9900 Series Intelli power X-ray Analyzer	Thermoscientific USA
Oxygen Bomb Calorimeter	Power-50- 60 Hz 90 - 260 VAC; Operating Temperature- 0-60 ^{0}C; Resolution- 0.001 MJ/Kg	XRY -1A	Shanghai Changji China
Muffle Furnace	Naberthern GmbH 300-3000 ^{0}C	LHT 406GN2G	Naberthern Company Germany
Weighing Balance	Mettler Toledo 0.01g – 110 g	AL 104	Mettler Toledo UK
Weighing Balance	0.5g – 3200 g	BSA 3202S	Sartorious group China
Laboratory Test sieves	850-212 microns	BS 410-1:2000	ELE International UK

Table 3.1: Equipment and Apparatus used

Table 3.1: Equipment and apparatus used (continued)

Equipment/Apparatus	Specification	Model	Manufacture
Laboratory Test sieves	850-212 microns	BS 410-1:2000	ELE International UK
Air-Jet Sieve Shaker Machine		Hosakawa Alpine E200LS	Hosakawa Alpine Germany
Electrothermal Blast drying Oven	0 – 300 ^{0}C	GZX-GFMBS-1	DHG Shanghai Longyue Company China
Jaw Crusher	-	PE60X100	Wuxi Jianyi China
Ball Mill	Grinding mediums 100 kg Material size < 7 mm Loading capacity ≤ g Barred speed ≈ 45r/min Grinding time ≈ 3 min Net weight ≈ 300kg	SM-500	Wuxi Jianyi, China
Thermostatic Digital Hot Plate	Heating Power – 1000 W L20, W30, H12cm	DB IIIA	Jiangsu Jinyi Tech., China
pH Meter	0.0 – 14.00 pH mV Range -2000 – 2000 Temp 0 – 100 ^{0}C	InLab (R)	Mettler Toledo, UK
Platinum Crucible	Platinum R=3D, H=1.1, B=0.6D	Pilab-200	Parekh Industries Ltd., Mumbai India
Compacting Machine			
Vicat Apparatus	Slide probe of 300 g, consistency plunger of 10 mm, diameter glass base plate. **Weight**: 5 Kg approx.	E0559N	Made in China
Automatic Cement Compressive/Flextural Machine	Class 1 Measuring Range:2.5 to 300 kN; 0.5 to 15 kN; 2.5 to 250kN. Power: 1000W, Maximum working pressure: Compressive-125bar, Flextural-30 bar	Toni Technik DIN 55220	Made in Germany
Prism Moulds	40x40x160	AIC-PRM-4416	AIC Lab Ltd India

Vials	240 mL	Fisher Scientific	Made in India
Humidity Cabinet and curing tank			

3.1.1 Sample preparation

The clinker samples were collected from Obajana cement plant Obajana Kogi State, which is one of the foremost indigenous cement companies in Nigeria one of the foremost indigenous cement companies in Nigeria. The sample collected was sieved through a 10 mm mesh size and retained on a 5 mm mesh size in order to determine the liter weight. A representative sample was also collected in order to determine the sample composition and the clinker free lime. The limestone sample also collected from Iwa-Oyo was grounded to reduce the size using a jaw crusher and then milled into fine powder. Sample weight of 1 g milled was taken for loss on ignition (LOI) while 5g of the raw sample was milled with ethylene glycol pellets and then pressed on a ring for analysis.

The Phosphogypsum sample was obtained from Senegal and then packed in plastic bags. The samples were then dried in an electric furnace at 105°C for at least four hours to constant weight, and then pulverized, homogenized and sieved into particles sizes ranged between 0.25 - 0.01mm using an automatic vibratory screen. The radiological assessment measured was below the maximum admissible concentration making it suitable for this research work (Djicknack *et al.*, 2018).

3.2 Methodology

3.2.1 Thermal treatment of phosphogypsum-clay mixture

The phosphogypsum sample was dried in an oven for 1 hour to remove the residual moisture present in the phosphogypsum. The phosphogypsum thermal treatment was carried out in a

high temperature furnace (Naberthern 3000) alongside the bentonite clay mixture at varying temperatures (up to 1000^0C), at a heating rate of 20°C/min for one hour. Partial decomposition of anhydrite gypsum begins at temperatures greater than 600 ^{0}C in phosphogypsum during its heating and is associated with the formation of lime (CaO) in the presence of acidic oxides (SiO_2 or Al_2O_3) with distinguished binding properties. The calcination of bentonite clay at temperatures between 500-600 ^{0}C also gives metabentonite as the resulting product.

3.2.2 pH determination of the heated products

Standard buffer solutions with established pH values that cover the measurement range are used to calibrate the pH electrode first. The heated product samples were pulverized into fine powder and dissolved in distilled water, then the electrode was inserted in the analyte until a constant value was obtained to determine the pH.

3.2.3 Microstructural characterization

3.2.3.1 *X-ray fluorescence (XRF) analysis*

X-ray fluorescence analysis is widely used to obtain chemical composition of all kinds of solid or liquid materials. Wavelength dispersive X-ray fluorescence spectrometry (WDXRF) is chosen due to its reliability and unrivaled accuracy of results. It is a powerful technique that has been used successfully to investigate various types of cement, polymers, mining, and industrial materials (Mayrhofer *et al.,* 2005). The chemical compositions of bentonite clay, phosphogypsum, and clinker samples in this research was determined using XRF. Approximately 10 g of each sample were grounded, pressed with ethylene glycol Tablets to stick to the rings and then scanned to determine their elemental compositions in this research.

3.2.3.2 *X-ray diffraction (XRD) analysis*

One of the most important tools is x-ray diffraction analysis which is used to identify,

categorize and quantify minerals (Williams and Carter, 2011). It has been extensively utilized to examine crystalline materials and cementitious products. The basic principle of XRD relies on diffraction of X-rays through the unique structures of crystalline materials (Mayrhofer *et al.,* 2005).

Approximately 10 g of each sample of phosphogypsum, and clinker samples were grounded, pressed with ethylene glycol Tablets to stick to the rings and then scanned to determine unique crystalline structure in this research.

3.2.2.3 *Scanning electron microscope/energy dispersive spectroscopy (SEM/EDX) analysis*

Scanning Electron Microscopy (SEM) is high vacuum equipment, since under a high vacuum fewer electrons can be dispersed, allowing for higher resolution images. The samples were pulverized and gently dried in a temperature-controlled oven at approximately 60 °C for 24 hrs before being coated by a sputtering process on a carbon fiber covered steel sample holder.

3.2.4 Determination of sulphite (SO_3) for gypsum purity

Gypsum sample of one gram was placed in a 250 mL flat bottom beaker and combined with ninety milllitre of distilled water. The mixture was heated with 10 mL of 0.1 M (35.4 percent % purity) concentrated hydrochloric acid until the sample was completely decomposed. After cooling, the solution was filtered using Whatman filter paper grade 40 into a 400 mL beaker. The filtrate was prepared up to 250 mL and then warmed till it reached boiling temperature. 10 mL of 0.5 molar $BaCl_2$ was added to the boiling solution while it was still boiling. For proper sulphate ion precipitation, the solution was allowed to cool for one hour with little disturbance.

The filtrate was filtered using Whatman grade 42 filter paper and washed in boiling water

until it was free of Cl^- ions. The lack of Cl^- ions was confirmed using silver nitrate. The residue (precipitate) was weighed in a porcelain crucible, blackened, and fired at 900°C for 30 minutes in a muffle furnace. After cooling in a desiccator, the residue was weighed. The weight difference was expressed as the sulphite composition as given in Equation (3.1).

$$\%SO_3 = \frac{mass\ of\ BaSO_3 \times 0.343}{mass\ of\ test\ sample} \times 100\% \quad (3.1)$$

Where 0.343 is the molar ratio of SO_3 to $BaSO_4$ or gravimetric factor of SO_3.

3.2.4.1 *Determination of gypsum purity*

The residue (precipitate) from the sulphite analytical determination was measured in platinum crucible, and burnt in a muffle furnace at 900°C for 30 min at a heating rate of 20°C per minute. The residue was dried in a desiccator, and the weight difference was used to calculate the sulphite (SO3) content.

Gypsum purity was then obtained by multiplying the percentage SO_3 by 2.15. Where, 2.15 is molar ratio of $CaSO_4.2H_2O$ to SO_3 (Appendix 2).

3.2.5 Preparation of laboratory cements for physio-chemical analysis

Standard methods were used for analyses of laboratory ordinary Portland cement and limestone composite by milling varying quantities of clinker, limestone and a quantity of gypsum with the aid of a laboratory cement ball mill, till the desired particle size and Blaine were attained. The cement blend was sieved through 1mm mesh. The samples are then stored in polyethylene bags to prevent hydration.

3.2.5.1 *Determination of loss on ignition (LOI)*

A sample weight of 1g of limestone sample (m_1) was introduced into an empty crucible and

placed in a muffle furnace at a heating rate of 20 ^{0}C per minutes for 30 min until it reaches 900 ^{0}C. As the furnace reaches the required temperature, the sample was timed and then removed after the required minutes and later allowed to cool by keeping in a desiccator and the value recorded as (m_2). LOI was computed as a percentage of m_1 according to Equation (3.2).

$$\text{LOI} = (m_1 - m_2) \times 100\% \quad (3.2)$$

Where m_1 and m_2 is the initial and final weight of the sample before and after ignition

3.2.5.2 ***Determination of free lime in clinker***

A sample weight of 0.750 g was measured in a 250 mL conical flask and 40 mL of ethylene glycol were added. The mixture was heated to 70 ^{0}C for 30 min in a water bath, and was filtered into a dry Erlenmeyer flask with a Gooch crucible having asbestos bed with the aid of a suction pump. The filtrate was titrated with 0.1 molar hydrochloric acid (HCl) using bromocresol green indicators. The titre value gotten was multiplied against the factor obtained to get the free lime content

$$Free\ lime = volume\ of\ 0.1M\ HCl \times 0.2804\ \% \quad (3.3)$$

3.2.5.3 ***Determination of water demand and consistency***

The volume of water weighing 225 ml using a measuring cylinder (*Wg*) were mixed with 450 g of cement sample within a maximum time of 4 min to make a paste. The resulting paste was put into a Vicat mould until it was full using a hand trowel. The mould was placed under the Vicat plunger, which weighed 300 g. The plunger was gradually lowered until it made contact with the paste's surface, and then allowed to penetrate the paste. The amount of water contained in the very paste which was allowed a penetration of 5-7 mm is taken as the water demand in accordance with NIS 444-1:2003 46. The consistency was then calculated using

the formula

$$C = \frac{w_g}{500g} \times 100\% \quad (3.4)$$

Where Wg is weight of water

3.2.5.4 ***Determination of setting time***

The cement paste that has gone through standard consistency test was transferred into an open mould on the base plate of the Vicat instrument by lowering the needle to settle on the instrument's base plate and then setting the pointer to zero on a graduated scale attached to the instrument. The needle was allowed to pierce the paste vertically. When the penetration stopped, the Vicat instrument's scale was read and the time was recorded. as the initial setting time, T_0.

The mould was later inverted, and the needle was attached with a ring, and allowed to rest on the reverse face of the paste. The final setting time T_f was recorded as that time, starting from onset of experiment when the ring failed to make a mark on the reverse surface.

3.2.5.5 ***Determination of soundness***

Cement paste of standard consistency was used to fill a Le Chatelier mould, which has two indicator needles. After filling the mould, the distance (d_o) in millimeters, between the needles was measured and recorded. The filled Le Chatelier mould was heated in boiling water for 30 min, and after staying in a humidity cabinet for 24 h, the soundness was later determined by measuring the new distance (d_f) between the two needles. The soundness was obtained by the difference,

$$\text{Soundness} = d_f - d_o. \quad (3.5)$$

3.2.5.6 ***Determination of cement residue using sieve method***

Cement sample weighing 100 g were sieved through 45 micrometer (μm), 90 μm and 180 μm sieves (BS 410). The residues were expressed as percentage of the initial weight.

$$\text{Residue} = \frac{mass\ of\ residue}{mass\ of\ sample} \times 100 \quad (3.6)$$

3.2.5.7 ***Determination of cement surface area using air permeability method***

Cement sample weighing 2.59 g was carefully introduced into an air permeability cell that has a filter paper on a disc with holes (1mm diameter) under it. The sample was covered by another filter paper disc on its top to avoid loss of material by sticking onto the surface of a plunger. A plunger was used to compact the sample, which was gently but firmly put into the cell until the plunger cap made contact with the cell. The cell was fitted into the manometer's socket at the top, and the manometer's stop clock was opened to change the liquid level to a lower etched line. The stop clock was released and the timer started automatically and it stopped when the liquid reached the upper etched line. The time for the liquid to move from the lower to the upper etched line was recorded as t_s.

Blaine (specific surface), or B is then calculated using Equation (3.7):

$$B = K\sqrt{t} \quad (3.7)$$

Where K is apparatus constant and B is in m^2/kg

To determine K, a reference sample of known B was compacted and subjected to air permeability test, and the time taken for the liquid to move from lower to higher etched line (tsav), was recorded. Afterwards K was obtained by the relationship;

$$K = \frac{B}{\sqrt{tsav}} \quad (3.8)$$

3.2.5.8 ***Determination of compressive strength***

The mortar was made out of one-part cement (450 g) and three parts standard sand (1350 g), with a water to cement ratio of 0.5:1 (225 g water). Water was placed into the bowl of a

mechanical mixer, and cement was gradually added to the water. The mixer was started on medium speed right away, and the grit was gradually added over the next 30 s. The mixer was set to great speed for another 30 s, following which it was shut off and the mortar was allowed to rest for 90 s. During the rest time, the sides of the mixer bowl were scrapped down to the bottom, before mixing resumed at high speed for another 60 s. The mortar samples produced were moulded immediately using a prismatic mould on a jolting apparatus (NIS 446-2003). The prismatic test specimens were manufactured in pairs for each mortar with the mould tightly attached to the jolting gear. The moulds were labeled accordingly and stored for 24 h in a humidity cabinet for the prisms to acquire strength enough to be demoulded without risk of damage (Sadique and Coakley, 2016). The compressive moulds is prepared is presented in Plate X before being placed in a curing tank for the 2 days, 7 days and 28 days compressive strength determination.



Plate X: Compressive moulds

$$RF = \frac{F}{A} \quad (3.9)$$

Where F is highest load at fracture in Newtons and A is prism area.

3.2.6 Determination of heat of hydration (HOH)

3.2.6.1 *Preparation of cement sample for HOH*

Cement quantity of about 60 g and 24 mL of distilled water was mixed in a mixer for 4 min and afterward filled into 3 glass tubes/vials fixed with wax and stopped. The temperature of the mixing water was between 15 ^{0}C and 25 ^{0}C. The vial tubes were put away in a vertical situation at 21.1± 1 ^{0}C in a humidity cabinet until the time of test.

3.2.6.2 *Calibration of heat capacity*

A test solution trial of 2 molar (M) ± 0.05 nitric acid was made up from analytical reagent quality materials, alongside hydrofluoric acid of 40 % w/w analytical reagent quality zinc oxide solution capacity. The heat capacity of the calorimeter was re-decided whenever a new batch is prepared.

3.2.6.3 *Determination of heat capacity*

The calorimeter was assessed after which 9.6 ± 0.1 mL of hydrofluoric acid and 388 ± 0.1 of 2M nitric acid was then estimated and poured into the calorimeter at a temperature of 18 ± 0.5 ^{0}C. The hydrofluoric acid was estimated in a little estimating chamber made up via fixing at 15 cm length of 2 cm distance across polythene pitch cylinder to a level plate of similar material through a little gas latch.

Enough zinc oxide weighing around 42 g was ignited for 1 h at 900-950 ^{0}C, cooled in a desiccator containing anhydrous calcium chloride and ground to go through a 60-mesh B.S.

sieve for six determinations. 7.0 g of this ignited oxide was again heated to 900-950 ^{0}C for 5 min, and was then cooled for not less than two and half hours and not over five hours in the calcium chloride desiccator prior to weighing precisely.

The calorimeter was assembled and the stirrer ran for3 at least 5 min to permit the temperature to get uniform. The temperature value was then recorded every five min and rectified to 0.001 ^{0}C to decide the underlying heating or cooling amendment. The zinc oxide was presented through the channel consistently over a time of 1-2 min; the pipe was then being brushed clean with a camel hairbrush.

The temperature values were taken at 1 min intervals until the solution is completed, as demonstrated by a consistent rate of heating or cooling of the calorimeter for a time of twenty min. Readings was proceeded for a further 5 min to decide the last heating or cooling redresses.

These corrections were summed and the total added or subtracted as appropriate to the observed temperature rise.

The heat capacity (C)

$$C = wt\ of\ ZnO(g)[256.1 + 0.1(30.0 - \theta) + 0.1(\theta_0 - \theta)] \qquad (3.10)$$

Where 256.1 is heat of solution of zinc oxide at 30 ^{0}C the first 0.1 is the negative temperature coefficient of the heat of solution, θ is the end temperature of the calorimeter and contents in centigrade degrees, the second 0.1 is the specific heat of zinc oxide and θ_0 is room temperature.

This expression simplifies to: -

Heat capacity (C) (Joule/kelvin) = Corrected temp. Rise

$$C = [wt\ of\ ZnO(g)[259 - 0.2\theta + 0.1\theta_0] \quad (3.11)$$

3.2.6.4 ***Determination of heat of solution of unhydrated Cement***

A sample of weight of 3 g of anhydrous cement was weighed out for the heat of solution, and also approximately 7 g was weighed out simultaneously for the loss on ignition. All the weighing was made to the nearest 0.001 g after which the determination of the temperature rise is then carried out exactly as described for zinc oxide. The heat of solution calculated as follows:

$$Heat\ of\ solution\ \left(\frac{Cal}{g}\right) \text{of unhydrated cement} =$$

$$\frac{\text{Heat capacity x corrected temperature rise} - 0.2\ (\theta_0 - \theta)}{\text{Weight of sample corrected for ignition loss}} \quad (3.12)$$

Where 0.2 is the specific heat of unhydrated cement. The mean was taken of three determinations carried out within 7 days of the mixing of the hydrated samples.

3.2.6.5 ***Determination of heat of solution of hydrated cement***

During the determination of heat of solution of hydrated cement, one of the glass sample tubes was broken and all follower wax and glass eliminated from the cement, which was then being ground (as quickly as conceivable to avoid carbonation) to pass an 18-mesh B.S. sieve. The ground sample was kept in a stoppered weighing bottle from which tests of 4.2 g and 7.0 g for heat of solution and loss on ignition (LOI) individually were taken. A loss on ignition was carried out 3.on each example utilized for heat of solution. The determination of the temperature rise was completed, and the heat of solution was calculated as follows:

Heat of solution of hydrated cement in calories per gram ignited weight =

$$Heat\ capacity\ \left(\frac{J}{k}\right) \text{corrected temperature rise} - 0.4(\theta_0 - \theta) \quad (3.13)$$

Weight of sample corrected for ignition glass Where 0.4 is specific heat of hydrated cement.

The mean was taken of three determinations on separate specimen tubes.

CHAPTER FOUR

4.0 RESULTS AND DISCUSSION

4.1 X-Ray Fluorescence Analysis

4.1.1 XRF analysis of the clinker Sample

Table 4.1 shows the various compositions of the parent clinker sample compositions, which was characterized in terms of chemical and mineralogical properties. The mineralogical properties are $3CaO.SiO_2$ or (C_3S), $2CaO.SiO_2$ or (C_2S), $3CaO.Al_2O_3$ or (C_3A) and $4CaO.Al_2O_3.Fe_2O_3$ or (C_4AF). Parameters shown in Table 4.1 indicated that the clinker is good for high quality Portland cement having gotten the free lime content of 1.35 % which indicates that there was proper reaction of lime with the oxides to form the mineral compounds. Furthermore, cement made from the clinker will most likely be sound and will have expansion of less than 10 mm as specified by NIS when hardened. Good clinker is expected to contain at least 55 % C_3S and not less than 70 % sum of C_2S and C_3S (Leon-Rena *et al*., 2009). The C_3S and C_2S values obtained are responsible for both the early strength and later strength in cement by forming calcium sulphate hydrate C-S-H and portlandite. The C_3S reacts fast while the C_2S reacts more slowly. The C_3A is responsible for the setting of cement as it acts a flux by reducing the burning temperature of clinker thereby facilitating the combination of lime and silica to form calcium silcate aluminate C-S-A. C_4AF reacts more slowly and is responsible for the grey colouration of the cement (Irassar, 2009).

Table 4.1 Chemical and mineral parameters of clinker parent sample

Chemical composition		**Mineral composition**	
Chemical content	**% Content**	**Mineral content**	**% Content**

SiO_2	21.09 ±0.06	C_3S	65.75
Al_2O_3	5.50 ±0.02	C_2S	13.81
Fe_2O_3	3.65 ±0.02	C_3A	8.81
CaO	65.17 ±0.04	C_4AF	11.63
SO_3	0.63 ±0.01	Litre Weight (g/L)	1260±0.58
MgO	1.10		
K_2O	0.30		
Na_2O	0.02	-	-
Free lime	1.35 ±0.01		
LOI	1.19 ±0.02	-	-

4.1.2 XRF analysis of phosphogypsum sample

The x-ray fluorescence of the phosphogypsum sample, and the mean sulphite content is presented in Table 4.2. The sulphite content from the wet chemical analysis of the PG was obtained to be 43.64%, while that obtained using XRF analyzer was 42.52%. The sulphite content of gypsum is directly related to its purity; indicating that high sulphite content indicates high purity.

The percentage purity of the phosphogypsum is calculated using Equation (29).

$$\% \text{ Purity} = \% SO_3 \text{ multiplied by } 2.15 \quad (29)$$

The percentage purity of the phosphogypsum was calculated to be 93.83% indicating high gypsum purity, since gypsum having more than 80% as $CaSO_42H_2O$ is considered suitable for maintaining SO_3 (Singh, 2003)

The main chemical components of the PG before and after treatment was analyzed using XRF machine as well as the maximum and minimum allowable limits as presented in Table

4.2. The elemental analysis of the treated PG in contrast to that of the natural gypsum shows that the values obtained are well below the regulatory limits which justify the performance of the thermal purification (Ajam, 2010). The analytical results showed a better reduction of phosphorous oxide (P_2O_5) from 1.05% to 0.38 % and fluorine from 2.22% to 1.25% by thermal treatment of the PG (Van-Der-Merwe and Strydom, 2004).

Table 4.2: Main Chemical Components of the PG before and after treatment

Constituents (wt. %)	Raw PG	Treated PG	Phosphogypsum Min - Max
CaO	44.90	46.28	28 - 45
SO_3	43.64	44.63	39 - 47
SiO_2	5.65	5.82	0.5 – 6.0
P_20_5	1.05	0.38	0.05 – 1.4
K_20	1.52	0.68	0.01 – 0.80
Al_2O_3	0.65	0.80	0.02 – 0.85
MgO	0.37	0.36	0.05 – 0.40
F	2.22	1.05	$\leq$ 1.5

4.1.3 XRF of the bentonite Clay

The bentonite clay used in the course of carrying out this experiment is analyzed using XRF equipment and the composition of the bentonite clay is presented in Table 4.3. The result of the XRF chemical composition of the bentonite clay presented in Table 4.3 indicates a very high silica content (SiO_2). The silica content of the clay was 67.82%, which revealed that the clay was more of a bentonite material as it had higher silica to alumina ratio of 2:1 (Rodriguez *et al*., 2015).

Table 4.3: XRF analysis of the Bentonite clay

Composition	SiO_2	Al_2O_3	Fe_2O_3	CaO	MgO	Na_2O	MnO	K_2O	LOI
Weight (%)	67.82	12.88	10.64	0.36	1.50	0.15	0.14	0.15	6.36

4.2 Microstructural Analysis using SEM/EDS

The morphology using SEM/EDS image analysis coupled with EDS atomic composition of the raw phosphogypsum particles is presented in Figure 4.1. The raw PG sample showed the presence of agglomerates in rhombic form and others in hexagonal form as shown in Figure 4.1. Its semi quantitative composition analyzed by SEM-EDS showed high contents of Ca, S, O and impurities such as P, Si, Na and F. The elemental composition of the raw phosphogypsum, depicted in Figure 5, shows that the particles exhibit different shapes: hexagonal, rhombic and needles, composed mainly of calcium and sulphur with the presence of phosphorous, silicon, sodium and fluorine impurities. By comparing the SEM-EDS analysis of the raw phosphogypsum samples, the presence of well-shaped needles and rhombic shapes was identified. According to Bennis *et al*., 2010, studying the synthesis and the formation mechanisms of previous works of $CaHPO_4.2H_2O$, showed the presence of needles and rhombic-shaped for this phase.

The SEM analysis of the treated phosphogypsum in Figure 4.2 shows new silica and alumina rich products such as amorphous calcium silicate hydrates (C-S-H) and calcium aluminate hydrates (C-A-H), including crystalline phases of phosphogypsum dihydrate crystals which fill and intertwine with each other to form a more compact structure with a mean particle size of 2,980.3 µm. Thermal treatment of phosphogypsum with bentonite clay yield amorphous

cementitious phases associated with strength enhancement, since C-S-H and C-A-H is co-existing products of the polymerization process (Chaunsali and Peethamparan, 2011).

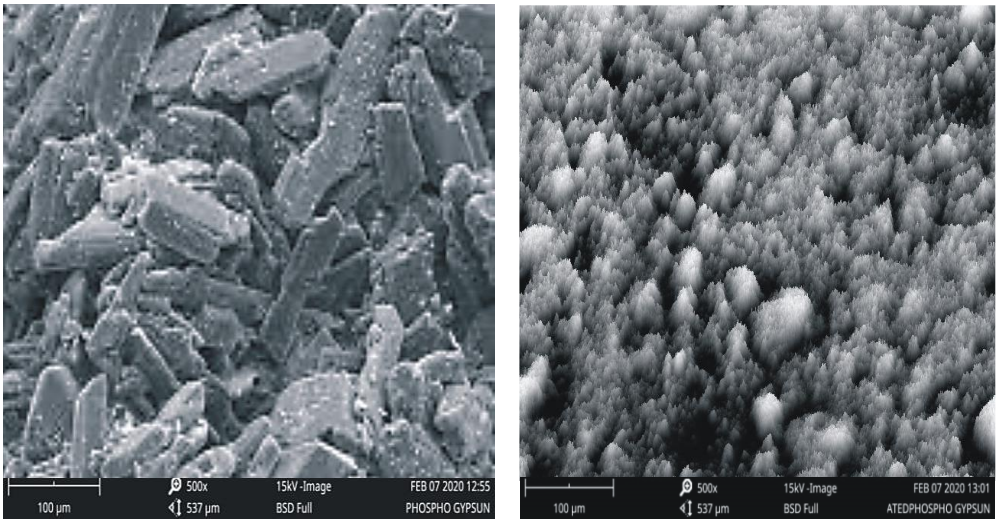

(a) (b)

Figure 4.1: SEM micrograph of (a) Raw Phosphogypsum (b) Treated Phosphogypsum

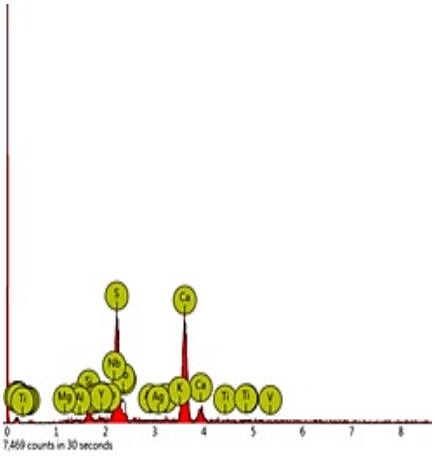

Element Number	Element Symbol	Element Name	Weight Conc.
20	CaO	Calcium	44.90
16	SO_3	Sulfur	41.64
14	SiO_2	Silicon	4.15
41	Nb_20_5	Niobium	1.94
39	Y_2O_3	Yttrium	1.57
47	Ag_2O	Silver	1.18
15	P_20_5	Phosphorus	1.05
23	V_20_5	Vanadium	1.02
19	K_20	Potassium	1.02
13	Al_2O_3	Aluminium	0.65
22	TiO_2	Titanium	0.51
12	MgO	Magnesium	0.37

(a)

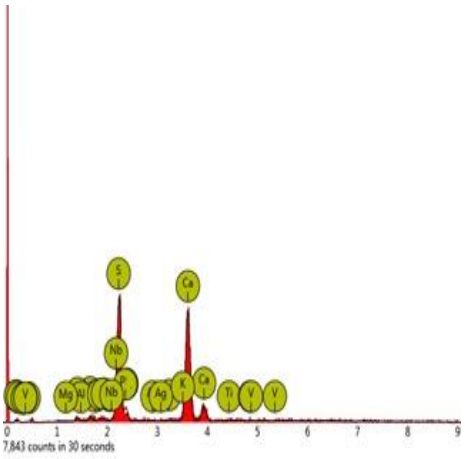

Element Number	Element Symbol	Element Name	Weight Conc.
20	CaO	Calcium	45.32
16	SO_3	Sulfur	43.46
39	Y_2O_3	Yttrium	1.70
41	Nb_20_5	Niobium	1.04
47	Ag_2O	Silver	0.87
13	Al_2O_3	Aluminium	0.80
14	SiO_2	Silicon	5.76
19	K_20	Potassium	0.67
15	P_20_5	Phosphorus	0.38
12	MgO	Magnesium	0.00
22	TiO_2	Titanium	0.00
23	V_20_5	Vanadium	0.00

(b)

Figure 4.2: EDS analysis of (a) Raw Phosphogypsum (b) Treated Phosphogypsum

4.3 X-Ray Diffraction Pattern of the Clinker and Phosphogypsum

The clinker and phosphogypsum samples were analyzed through X-ray diffraction (XRD) to determine their crystalline composition (Waseda *et al*., 2011). The XRD analyses treated phosphogypsum samples was carried out to assess the effect of thermal treatment on its surface morphology.

4.3.1 X-Ray diffraction pattern of the clinker

XRD analysis was used to characterize clinker phases in order to identify distinct phases of the clinker sample as shown in Figure 4.2 and Table 4.4. The peaks of the clinker sample can be clearly observed and this shows the liquid phases of the X-ray diffraction pattern analysis; alite (C_3S), belite (C_2S), aluminate (C_3A), and ferrite (C_4AF) with percentage composition of 65.74, 11.63, 13.81 and 8.82 respectively. Good clinker is expected to contain at least 55 % C_3S and not less than 70 % sum of C_2S and C_3S (Leon-Rena *et al*., 2009).

This result indicates that the liquid phases C_3S, C_2S, C_3A, and C_4AF contents lies within the range recommended by the European standards specifications for ordinary Portland cement purposes (Waseda *et al*., 2011).

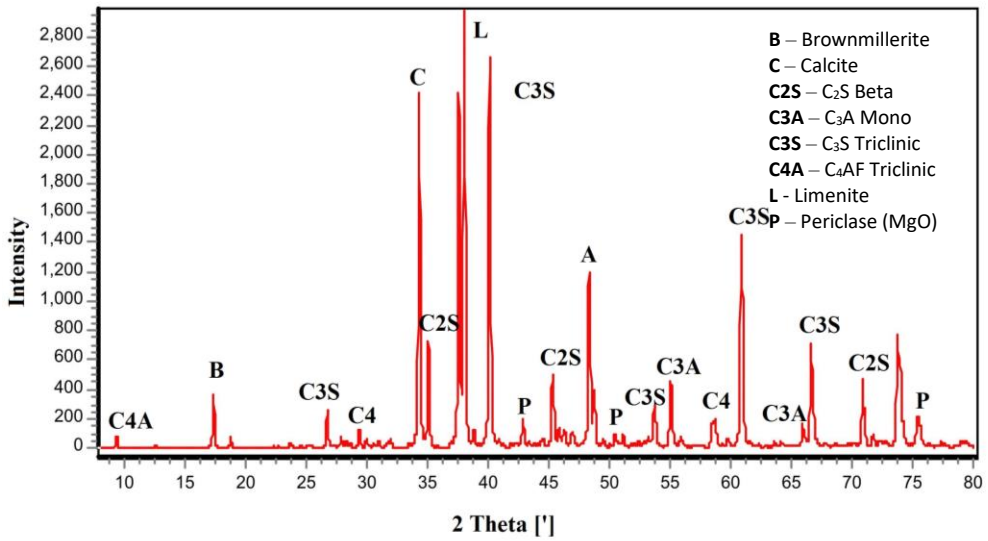

Figure 4.3: XRD analysis of clinker sample

Table 4.4: Compound composition of clinker phases analyzed

Compound Composition	**% Composition**
C_3S (Belov)- Alite)	65.74
C_2S (Alpha) - Belite)	11.63
C_3A (Mono) - Celite	13.81
C_4AF - Brownmillerite	8.82

4.3.2 X-Ray Diffraction pattern of the phosphogypsum sample

The peaks registered by the phosphogypsum sample is presented in Figure 4.3 and Table 4.5 to recognize different phases (crystalline and amorphous phases) within the phosphogypsum sample. All the diffraction peaks displayed in the XRD pattern were easily indexed to pure hexagonal and rhomboid structure according to Joint Committee on Powdered Diffraction Standard (JCPDS) card for gypsum (JCPDS:09-0432). The flat line of 2θ ranging from 10-30^0 signifies crystalline phases.

In Figure 4.3, the aggregate mass of rhombic shaped particles that looked to have been generated by many flaky particles stacked together in the form of agglomerates can be seen in the raw phosphogypsum peaks. During the heating of phosphogypsum and bentonite mixes at 200-1000 ^{0}C, the X-ray diffraction pattern analysis revealed the following peaks. The phosphogypsum decomposition product anhydrite include; quartz from bentonite decomposition products; SiO_2 from cristobalite and other anhydrite and bentonite interaction

products such as alite (C_3S), belite (C_2S); tri-calcium aluminate (C_3A), and tetra-calcium alumino ferrite (C_4AF). The quantification of the liquid phases for the phosphogypsum and clay mixture (PGC) indicated that the value of the C_3S in it is up to the required value (Leon-Rena *et al*., 2009). The PGC heated shows the presence of a significant amorphous phase including crystalline phases of gypsum dihydrate crystals (Scarlett and Madsen, 2006).

This result indicates that the liquid phases C_3S, C_2S, C_3A, and C_4AF having a percentage composition of 50.6, 21.8, 14.4 and 13.2 respectively lies within the range recommended by the European standards specifications for ordinary Portland cement purposes thereby, making treated phosphogypsum suitable to be use as a substitute for natural gypsum (EN 197-1, 2000).

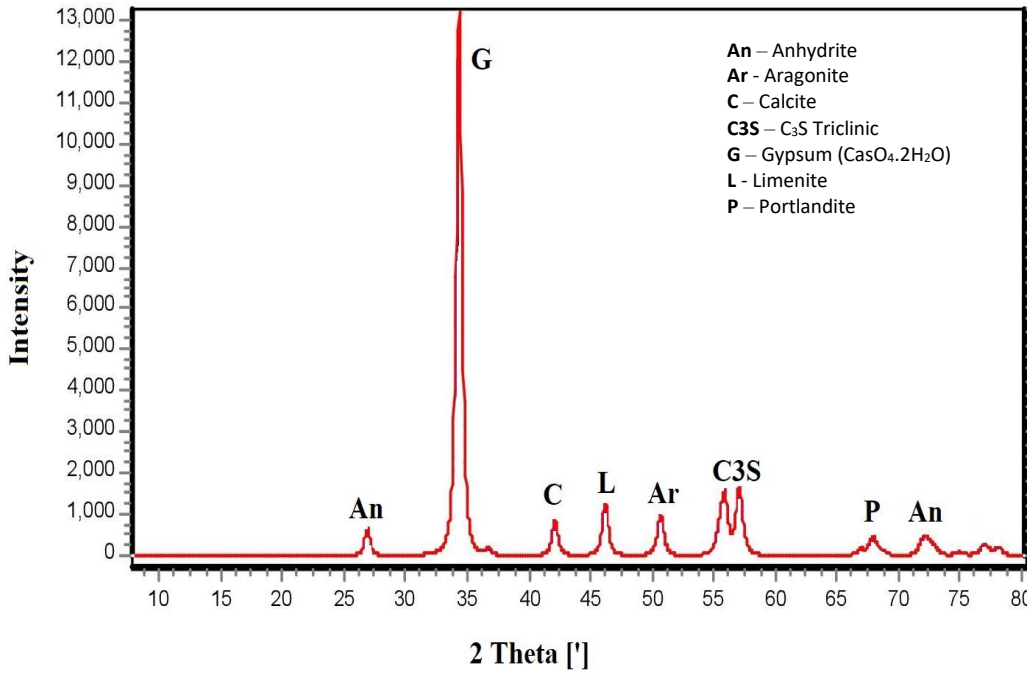

Figure 4.4: XRD analysis of the heated phosphogypsum

Table 4.5: Compound composition of treated phosphogypsum phases analyzed

Compound Composition	% Composition
C_3S (Belov) - Alite	50.6
C_2S (Alpha) - Belite)	21.8
C_3A (Mono) - Celite	14.4
C_4AF - Brownmillerite	13.2

4.4 Physical Analysis of the Portland Cement Produced

The various temperatures at which each of the mixture of PG and bentonite clay (PGC) products are heated in the furnace and also the physical analysis of the Portland cement produced is presented in Table 4.6. The various temperatures at which each of the mixture of PG and bentonite clay (PGC) products are heated in the furnace ranging from 200-1000 ^{0}C is presented as well as the physical analysis of the Portland cement produced which encompasses: Blaine, sulphur content, loss on ignition (LOI), the standard consistency, and pH metric analysis. The pH analysis of the phosphogypsum saturated solution samples showed an increase in pH value, as a result of decomposition of the heated product also, the Blaine values gotten are in accordance with the set target ($\geq$4500 cm^2/g). The Physical testing carried out on the PGC cement produced in Table 4.6 shows that the values obtained for the

blaine, sulphur value and standard consistency are in line with the optimum quality parameters for CEM II (Al-Hwaiti, 2013).

Table 4.6: Physical Analysis of the Portland cement Produced

Product	**Gypsum Temp (^{0}C)**	**Heating Time (S)**	**Heating Rate (^{0}C)**	**Blaine (cm^2/g)**	**SO_3**	**LOI**	**Normal Consistency (mL/g)**	**pH Analysis**
PGC 1	200	3600	10	4720	2.23	7.20	27.0	4.31
PGC 2	300	3600	10	4850	2.27	7.01	27.5	4.78
PGC 3	400	3600	10	4900	2.39	6.89	28.0	4.92
PGC 4	500	3600	10	4655	2.11	6.66	28.0	5.08
PGC 5	600	3600	10	4510	2.16	7.11	28.0	6.12
PGC 6	700	3600	10	4550	2.13	6.85	28.0	6.85
PGC 7	800	3600	10	4830	2.25	7.17	28.0	8.11
PGC 8	900	3600	10	4790	2.21	7.08	28.0	8.23
PGC 9	1000	3600	10	4825	2.34	6.93	28.0	8.84

The heated temperature, compressive strength and setting time of the Portland cement produced using

PGC is shown in Table 4.7. The compressive strength was found to be higher in treated condition than the untreated condition. From Table 4.7, the products did not set at all at lower temperatures of 100-300 ^{0}C, but gradually improves as temperature increases until optimum at 700 ^{0}C, and then decline at very high temperatures. For both the initial and final setting times, the processed sample recommended a 10% addition (comparable with control sample). It could be inferred that the heated products at 700 ^{0}C has the optimum values in terms of strength development and also the setting time was within range as shown in Table 4.7. In other words, it signifies that it may not necessarily require heating the PGC to a very high temperature to get the best performance, since it is imperative to minimize cost while maximizing profit. Heating the PGC to a temperature above 600 ^{0}C decontaminates and removes the obstruction admixtures that impair PG strength formation. The compressive strength values of regular Portland cement samples incorporating treated phosphogypsum after 2 days, 7 days, and 28 days are consistent with the OPC specification found in Nigerian Industrial Standard (Oyenuga, 2014). It can be concluded that the compressive strength has sufficient strength for ordinary Portland cement operations.

Table 4.7: Setting Time and Compressive Strength Analysis of the Portland cement

Temperature For 1 H (5% Heated Phosphogypsum) Cem II OPC						
Products	**Heated Temperature (^{0}C)**	**IST**	**FST**	**2 Days Avg**	**7 Days Avg**	**28 Days Avg**
PGC1	200	430	NOT SET	16.8	27.9	40.4
PGC2	300	410	NOT SET	18.4	33.6	41.7
PGC3	400	335	410	18.6	34.8	45.6

PGC4	500	250	405	21.5	35.6	46
PGC5	600	205	355	24.5	37.3	46.6
PGC6	700	195	245	24.4	36.3	48.6
PGC7	800	165	240	25.2	39.2	47.5
PGC8	900	165	245	25.0	38.8	47.2
PGC9	1000	185	240	23.0	39.0	47.0

The compressive strength of the cement produced using thermally treated PG as compared with National Industrial Standards (NIS) is presented in Table 4.8. The Compressive strengths of treated PG at 2 days, 7days and 28 days have adequate strength for ordinary Portland cement (OPC) applications. Thermal treatment of phosphogypsum and integration of bentonite clay conforms and meets the requirements obtained in Nigeria Industrial standard (NIS 446:2003).

Table 4.8: Compressive Strength of the Standard Cement using Ordinary Gypsum and PG Portland Cement Produced.

COMPRESIVE STRENGTH (MPa)						
	NIS Standard Requirement for Ordinary Gypsum Portland Cement			**Experimental Values obtained for Heated Phosphogypsum Portland Cement**		
Product	**2D**	**7D**	**28D**	**2D**	**7D**	**28D**
CEM I (52.5)	≥ 20	≥ 44	≥ 52.5	27.5	48.5	63.5
CEM II (42.5)	≥ 20	≥ 33	≥ 42.5	25.8	35.8	46.0

These results were confirmed and fulfilled the requirement with the specification of OPC obtained in Nigeria Industrial standard (NIS 446:2003).

4.5 Heat of Hydration Analysis of the Portland Cement Produced

Table 4.9 shows the heat of solution for measuring the hydration enthalpy (HOH) of the phosphogypsum Portland cement using isothermal conduction calorimetry. The heat capacity of the equipment was determined to be 1,378 kJ/kg, and the heat of solution for the anhydrous and hydrated cement were determined and the difference taken to obtained the heat of hydration of the PGC cement produced. The amount of C_3S and C_3A in the cement influence the heat of hydration the most, but fineness, curing temperature, and the water-cement ratio also have a role. As each of these factors is enhanced, the heat of hydration increases. The heat of hydration value of 180.66kJ/kg and 294 kJ/kg obtained for 2 days and 28 days respectively is in accordance with BS EN 196-9:2010 as given in Table 4.9. The value of 294 kJ/kg obtained is in accordance and also meets the requirement for ordinary Portland cement according to ASTM C 150 (2009), which requires a maximum of 290 J/g for type II (OPC) cements.

Table 4.9: Heat of hydration for the PG cement sample produced

DAYS (D)	**Heat Capacity of Equipment (C) (kJ/kg)**	**Heat of Solution of Anhydrous Cement (kJ/kg)**	**Heat of Solution of Hydrated Cement (kJ/kg)**	**Heat of Hydration (HOH) (kJ/kg)**	**Heat of Hydration (HOH) (cal/g)**
7	1,378	1,660.730	1,480.070	180.660	43.180

28	1,378	1,660.730	1,366.280	294.450	70.370

CHAPTER FIVE

5.0 CONCLUSION AND RECOMMENDATIONS

5.1 Conclusion

In this study, the laboratory results obtained showed that the pH analysis of the value of phosphogypsum saturated solution samples increased, as a result of decomposition of the heated product. The SEM-EDS examination of the raw phosphogypsum sample revealed the existence of aggregates in tabular and hexagonal shapes. The treated phosphogymsum samples fill and intertwine with each other to form a more compact structure.

The sulphite content of the heated phosphogypsum was 43.64%, which translates to a purity of 93.83 % also, the free lime content of 1.35 % indicates that there was proper reaction of lime with the oxides to form the mineral compounds. The phosphorous and fluoride content reduced appreciably from 1.05 mg/L to 0.38 mg/L and 2.22 mg/L to 1.05 mg/L respectively

for the raw and treated PG. The compressive strength of the Portland cement produced was also found to be higher than in the treated state, due to the removal of the binding obstruction admixtures by thermal treatment of the PGC.

The heat of hydration value of 180.66kJ/kg and 294 kJ/kg obtained for 7 days and 28 days respectively is in accordance with BS EN 196-9:2010. The laboratory tests performed in this study indicated that phosphogypsum could serve as a replacement of natural gypsum as a set retarder because thermal treatment of phosphogypsum significantly removed the impurities present effectively, allowing it to be used as a replacement of natural gypsum in the manufacturing of Portland cement.

5.2 Recommendations

1. Research study can be further carried out to determine the performance of phosphogypsum utilizing plasticizers in strength development in concrete works.
2. Also, the kinetic study of the phosphogypsum treatment can be explored to determine exact heating temperature for obtaining an expected amount of lime (CaO) in the product that can be calculated according to the given thermodynamic Equation with respect to the rate of treatment to ascertain optimum temperature for improved performance.

5.3 Contribution to Knowledge

1. Thermal treatment of phosphogypsum-clay interaction reduced the phosphorous and fluoride content appreciably from 1.05 mg/L to 0.38 mg/L and 2.22 mg/L to 1.05 mg/L respectively, thereby making it serve as a replica for natural gypsum.
2. Inertisation and stabilization of phosphogypsum using high temperature furnace revealed that at a temperature above 550 ^{0}C there was removal of the obstructive admixtures, giving optimum setting time of 240 mins and compressive strength of 63.5 MPa and 46.0 MPa for CEM I (52.5) and CEM II (42.5) Portland cement respectively.
3. Thermal reaction of phosphogypsum containing calcium oxide with bentonite clay gave values of 50.6%, and 21.8% for C_3S and C_2S respectively with distinguished binding properties and enhanced strength development.

REFERENCES

Abramov, A. M., Galieva, Z. N., Galiev, R. S., Sabinina, O. R., & Sobol, J. B. (2013). Method for extracting rare earth metals from phosphogypsum. *Journal of Cleaner Production*, 10, 46-48.

Abushad, M., & Sabri, M.D. (2017). Comparative Study of Compressive Strength of Concrete with Fly Ash Replacement by Cement. *International Research Journal of Engineering and Technology*, 4, 2627-2630.

Al-Hwaiti, M., Ross, P. & Ranville, J. (2013). Bioavailability and mobility of trace metals in phosphogypsum from Aqaba and Eshidiya, Jordan. *Journal of Environmental Geochemistry and health,* 70, 283-291.

Al-Jabbari S., Faisal F., Ali S., & Nasir S. (1988) The physical methods for purification of the phosphogypsum for using it as building material. *Journal of Building Research Sciences Resources* Council Baghdad 7,49–69

Aranda, M. A. G., De la Torre, A. G. & Leon-Reina, L. (2012). Rietveld Quantitative Phase Analysis of OPC Clinker. *Review of Mineral Geochemistry,* 74, 169–209.

Ayres R. U., Holmberg J., & Anderson B. (2001). Materials and the global environment: Waste mining in the 21st century, *Journal of Cleaner Production*, 26, 477-480.

Belboom, S., Szocs, C., & Léonard, A. (2015). Environmental impacts of phosphoric acid production using di-hemihydrate process: A Belgian case study. *Journal of Cleaner Production*, 108, 978-986.

Bennis, H., Benslimane, R., Vicini, S., Mairani, A. & Princi, E. (2010). Fibre width measurement and quantification of filler size distribution in paper-based materials by SEM and image analysis. *Journal of Electron Microscopy,* 59: 91-102.

BSI. 2003. BS EN 196-8: 2003, *Methods of testing cement-Heat of hydration-solution* British Standards Institution, UK.

Canut, M. (2006). Viability study for the substitution of gypsum by phosphogysum as a building material, Belo Horizonte, Federal University of Minas Gerais, Brazil.

Chang, P. K. (2004). An approach to optimizing mix designs for properties of high-performance concrete. *Cement and Concrete Research*, 34, 623-629.

Chaunsali, P., & Peethamparan, S. (2011). Evolution of strength, microstructure and mineralogical composition of a CKD-GGBFS binder. *Cement and Concrete Research,* 41, 197-208.

Chen J. J., & Kwan A. K. H. (2012). Superfine cement for improving packing density, rheology and strength of cement paste. *Cement and Concrete Composites*, 34, 1-10.

Degimency, Nurhayaton (2008) Utilization of phosphogypsum as raw and calcined material in manufacturing of building products. *Construction and Building Materials*, 8, 1857-1862.

Djicknack D., Modou M., Mamadou L. S., Cheikh A., Bamba D. & Ababacar S. N. (2018) Survey of activity concentration and dose estimation of naturally occurring radionuclides (^{232}Th, ^{238}U and ^{40}K) in the Coastal area of Dakar. *Indian Journal of Science and Technology*, 11, 6. DOI: 10.17485/ijst/2018/v11i40/131537.

Dunstetter F., de Noirfontaine M-N., & Courtial M., (2006) Polymorphism of tricalcium silicate, the major compound of Portland cement clinker. 1. Structural data: review and unified analysis. *Cemement Concrete Resources*, 36, 39–53.

Dunuweera S.P., & Rajapakse, R. M. G. (2017). Cement types, composition, uses, environmental impact and possible solutions, in Proceedings of the 28th International Symposium on Transport Phenomena, Peradeniya, Sri Lanka, September 2017.

Bennis, H., Benslimane, R., Vicini, S., Mairani, A. & Princi, E. (2010). Fibre width

measurement and quantification of filler size distribution in paper-based materials by SEM and image analysis. *Journal of Electron Microscopy,* 59, 91-102.

Edwards, P. (2011). 'Future Cement -Looking beyond Ordinary Portland Cement' -*Global Cement Magazine*, 12-22.

Erdogan Y., Ayhan D., & Hasan G., (1994). Partly-refined chemical by-product gypsums as cement additives. *Cement and concrete research*, 4, 601-604

Felhi, M., Tlili, A., Gaied, M.E., & Montacer, M. (2008). Mineralogical study of kaolinitic clays from Sidi El-Bader in the far north of Tunisia. *Applied Clay Science,* 6, 208-217.

Fertilizer (Control) Order, (2014). Published in the Gazette of India vide No. GSR 758 (E) dated the 25th September 1985 and latest amended vide No. S.O. 2886 (E) dated 3rd December 2014.

Gupta, V., Hampton, M. A., Stokes, J. R., Nguyen, A. V., & Miller, J. D. (2011). Particle interactions in kaolinite suspensions and corresponding aggregate structures. *Colloid Interface Science*, 359 95-103.

Hammas-Nasri, I., Horchani-Naifer, K., & Férid, M. (2016). Rare earths concentration from phosphogypsum waste by two-step leaching method. *International Journal of Mineral Processing*, 149, 78–83.

Harrisson A.M., (2014). The importance of raw materials. *International Cement Review*, 6,8.

Heiri, O., Lotter, A. F., & Lemcke, G. (2001). Loss-on-ignition as a method for estimating organic and carbonate content in sediments: reproducibility and comparability of results. *Journal of Paleolimnology*, 25, 101-110.

Kautz, C.Q. & Ryan, P. C. (2003). The 10 Å to 7 Å halloysite transition in a tropical soil sequence, Costa Rica. *Clays and Clay Minerals*, 51, 252-263.

Kazragis, A. (2004). High temperature decontamination and utilization of phosphogypsum. *Journal of Environmental Engineering and Landscape Management*, 4, 138-145.

Korsch, M., & Walther, W. (2015). Peri-implantitis associated with type of cement: a retrospective analysis of different types of cement and their clinical correlation to the peri-implant tissue. *Clinical Implant Dentistry and Related Research*, 17, e434–e443.

Kwon, W. T., Kim, Y. H., Chu, Y. S., Lee, J. K., Kim, I. S., & Kim, S. R. (2005). Effect of phosphorous and chloride on clinkering reaction. *Journal Material Online,* 1, 1-8.

Leon-Reina, L., De-la-Torre, A. G., & Porras-Vasquez, J. M. (2009). Round robin on Rietveld quantitative phase analysis of Portland cements. *Journal of Applied Crystallography*, 42, 906-916.

Liaqat, A. Q. & Saeed, A. (2011). Optimization of fineness of Ordinary Portland Cement Manufactured in Pakistan Mehran University. *Research Journal of Engineering and Technology*, 30, 549-558.

Mayrhofer, P. H., Mitterer, C., & Clemens, H. (2005) Self-organized nanostructures in hard ceramic coatings. *Advance Engineering Materials*. 7, 1071-1082.

Medeiros-Junior, R., & Lima, M. G. (2016). Electrical resistivity of unsaturated concrete using different types of cement. *Construction and Building Materials*, 107, 11-16.

Murray, H. (2002). Traditional and new applications for kaolin, smectite, and palygorskite: a general overview. *Application of Clay Science*, 17, 207-221.

Naik, T. R., Singh S. S., & Ramme, B. W. (2001). Time of setting influenced by inclusion of fly ash and chemical admixtures. *7th International Conference on Fly Ash, Silica Fume, Slag and Natural Pozzolans in Concrete (CANMET/ACI)*, 1, 393-413.

Nigeria Industrial Standards 444-1:2003, Cement-composition, specifications and conformity criteria for common cements.

Nigeria Industrial Standards 445:2003, Chemical analysis of cements.

Nigeria Industrial Standards 446:2003, Determination of strength of Portland cement.

Novotny, R., Bartoníþková, E., Švec, J., & Monþeková, M. (2016). Influence of active alumina on the hydration process of Portland cement. *Procedia Engineering*, 151, 80–86.

Okeowo, Alexis (7 March 2013). Africa's Richest Man, Aliko Dangote, Is Just Getting Started. *Bloomberg*. Retrieved 25 October 2016.

Oumnih, S., Gharibi, E. K., Yousfi, E. B., Bekkouch, N., & El-Hammouti, K. (2017). Posphogypsum waste valorization by acid attack with the presence of metallic iron. *Journal of Matererial Environmental Science*, 8, 338-44.

Oyenuga, V., 2014. Cement not Responsible for Building Collapse in Nigeria. An Editorial in This day Newspapers of 13th May 2014.

Punmatharith, T., Rachakornkij, M., Imyim, A., & Wecharatana, M. (2010). Co-processing of grinding sludge as alternative raw material in Portland cement clinker production. *Journal of Applied Sciences*, 10, 1525-1535.

Rashad, A. M. (2017). Phosphogypsum as a construction material. *Journal of Cleaner Production*, 166, 732-734.

Reeves, G. M., Sims, I. & Cripps, J. C. (2006). *Formation and alteration of clay materials.* Geological Society, London, Engineering Geology Special Publications. 21, 29-71.

Sadique, M., & Coakley, E. (2016). The influence of physico-chemical properties of fly ash and CKD on strength generation of high-volume fly ash concrete. *Advance Cement Research*, 28, 595-605

Singh, G. V. P. B., & Subramaniam, K. V. L., (2019). Production and characterization of low-energy Portland composite cement from post-industrial waste. *Journal of Cleaner Production*, 239: 118024. DOI: https:doi.org/10.1016/j.jclepro.2019.118024

Singh, M. (2003). Effect of phosphatic and fluoride impurities of phosphogypsum on the properties of selenite plaster. *Cement and Concrete Research,* 9, 1363-1369.

Singh, M. (2002). Treating waste phosphogypsum for cement and plaster manufacture. *Cement Concrete Research*, 32, 1033-1038.

Sparavigna, A.C. (2011), *Materials science in ancient Rome,* Archaeogate.

Van-der-Merwe, E.M., & Strydom, C. A., (2004). Purification of South African phosphogypsum for use as Portland cement retarder by combined thermal and sulphuric acid treatment method. *South African Journal of Science,* 100, 411-414

Waseda, Y., Toguri, J. M., Matsubara E., & Shinoda, K. (2011). Structure of silicate melts determined by X-ray diffraction, in Dynamic Processes of Material Transport and Transformation in the Earth's Interior, edited by F. Marumo. *Terra Scientific Journal Tokyo*, pp. 37-51.

Williams, D. B. & Carter, C. B. (2011). Transmission Electron Microscopy, vol. 1-4, Plenum Press, New York.

Won, J. S., Jacques, L., & Serge, L. (2012). The Effects of Salinity and Shear History on the Rheological Characteristics of Illite-Rich and Na-Montmorillonite-Rich Clays. *Clays and Clay Minerals,* 60, 108-120.

APPENDICES

APPENDIX A

Derivations of Constants

$CaSO_4.2H_2O \rightarrow CaSO4 + 2H_2O$

$CaSO_4 \rightarrow CaO + SO_3$

Theoretically,

$CaSO_4.2H_2O \rightarrow SO_3$

172 g/mol→80 g/mol

Therefore, $CaSO_4.2H_2O/SO_3 = 2.15$

Sulphate molar ratio

$CaSO_4.2H_2O \rightarrow CaSO_4 + 2H_2O$

$CaSO_4 + BaCl_2 \rightarrow CaCl_2 + BaSO_4$

$BaSO_4 \rightarrow BaO + SO_3$

233 g/mol → 80 g/mol

$(SO_3/ BaSO_4) \times 100 = 34.3\ \%$

Note that 34.3 is the molecular ratio of SO_3 to $BaSO_4$, otherwise known as the Gravimetric Equivalent.

Also note that % purity of SO_3 in gypsum is = % SO_3 (above) X 2.15

APPENDIX B

Preparation of Reagents and Indicators

Bromocresol green (BCG) indicator 1g BCG in 75mL Ethanol and made up to 100 mL with distilled water.

Buffer solution

35 g ammonium chloride was dissolved in 285 mL conc. Ammonia solution and made up to 500 mL with cold distilled water.

Phenolphthalein indicator 5 g of indicator was dissolved in minimum methanol and made up to 100 mL with distilled water.

APPENDIX C

CALCULATION OF HEAT OF HYDRATION OF THE PG CEMENT PRODUCED

Calculation of Heat Capacity of Calorimeter

Formula Used

$$C = \frac{M}{R} \times [1072 + 0.4(30 - t) + 0.5(T - t)$$

$$C = \frac{M}{R} \times [1084 - 0.9t + 0.5T$$

$R_0 = \Theta_{20} - \Theta_0$

$R = R_0 - (\Theta_{40} - \Theta_{20})$

Definition of Terms

C- Heat Capacity

M-Mass of zinc Oxide

R-Corrected Temperature rise

1072- Heat capacity of Zinc Oxide at 30^oC

0.4- Negative Temperature Coefficient of the heat of solution

0.5- Specific heat of zinc Oxide

t- Final temperature of the calorimeter and content in ^oC

T- Room temperature in ^oC

R_0=observed temperature rise, °C,

R = corrected temperature rise, °C, and

Θ_0= calorimeter temperature when sample was introduced,

Θ_{20} = calorimeter temperature at the end of the solution period

Θ_{40} = calorimeter temperature at the end of the correction period

Input Values

Θ_0	1.361
Θ_{20}	5.542
Θ_{40}	5.553
M	7.000
T	29.400
t	31.700

$R_0 = 5.542 - 1.361 = 4.181$

$R = 4.181 - (5.553 - 5.542) = 4.17$

$C = \frac{7}{4.17} \times [1084 - 0.9(31.70) + 0.5(29.40) = 1{,}738\ kJ/^0\text{C}$

Heat Capacity (C) of the calorimeter is 1,738 kJ/kg

Calculation of Heat of Solution (HOH) for the Anhydrous Cement

Formula Used

$$\text{H1} = \frac{\text{CR}}{\text{M}} - 0.8(\text{T} - \text{t})$$

Definition of Terms

C- Heat Capacity

0.8- the Specific heat of unhydrated Cement

R-Corrected Temperature Rise

M -Mass of the sample corrected For Ignition loss

t- Final temp. of the calorimeter and content in ^{o}C

T- Room temperature in ^{o}C

Θ_0,Θ_{20} and Θ_{40} retain their usual meaning

M1- mass of the sample based on Ignition loss

M1- mass of the sample based on Ignition loss

H1-Heat of Solution of unhydrated cement

Input Values	
Θ_0	2.0600
Θ_{20}	4.7300
Θ_{40}	4.7330
M	3.0000
T	29.800
t	31.000
C	1738.090
LOI (%)	6.910

$$\mathrm{H1} = \frac{\mathrm{CR}}{\mathrm{M}} - 0.8(\mathrm{T} - \mathrm{t})$$

$$R_0 = 4.750 - 2.060 = 2.790$$

$$R = 2.790 - (4.7500 - 4.7530) = 2.7875$$

$$H1 = \frac{1738 \times 2.7875 \times 100}{3 \times 93.09} - 0.8(29.80 - 31.00)$$

H1 = 1,660.73 kJ/kg

Calculation of Heat of Solution of Partially Hydrated Sample for 7 Days

Formula UsedDefinition of Terms

Where C, R, M, T &t retain their usual meaning as in anhydrous

1.7 is the Specific heat of hydrated Cement

H2- heat of solution of hydrated cement

Input Values	
Θ_0	1.850
Θ_{20}	4.480
Θ_{40}	4.483
M	4.180
T	30.00
t	32.00
C	1738.090
LOI	25.89

$$H2 = \frac{CR}{M} - 1.7(T - t)$$

$$R_0 = 4.485 - 1.850 = 2.635$$

$$R = 2.635 - (4.483 - 4.480) = 2.632$$

$$H2 = \frac{1738 \times 2.632 \times 100}{4.180 \times 74.11} - 1.7(29.50 - 32.00)$$

$$\boldsymbol{H2} = 1{,}480.07$$

Calculation of Heat of Hydration (HOH) of Cement produced for 7 Days

Definition of Terms

H1 Heat of solution of unhydrated cement

H2 Heat of Solution of partially hydrated cement

HOH Input Values (kJ/kg)	
H1	1,660.73
H2	1,480.07

HOH	**180.66**

Calculation of Heat of Solution of Partially Hydrated Sample for 28 Days

Formula UsedDefinition of Terms

Where C, R, M, T &t retain their usual meaning as in anhydrous

1.7 is the Specific heat of hydrated Cement

H2- heat of solution of hydrated cement

Input Values	
Θ_0	2.100
Θ_{20}	4.490
Θ_{40}	4.495
M	4.180
T	29.500
t	31.700
C	1738.090
LOI	27.220

$$H2 = \frac{CR}{M} - 1.7(T - t)$$

$$R_0 = 4.490 - 2.100 = 2.390$$

$$R = 2.390 - (4.490 - 4.495) = 2.385$$

$$H2 = \frac{1738 \times 2.385 \times 100}{4.180 \times 72.78} - 1.7(29.50 - 31.70)$$

$$\boldsymbol{H2} = 1{,}366.28 \text{ kJ/kg}$$

Calculation of Heat of Hydration (HOH) of Cement produced for 28 Days

Definition of Terms

H1 Heat of solution of unhydrated cement

H2 Heat of Solution of partially hydrated cement

HOH Input Values (kJ/kg)	
H1	1,660.73
H2	1,366.28
HOH	**294.45**

Where,

1cal/g = 4.184 kJ/kg

HEAT OF SOLUTION OF CEMENT SAMPLE	
$H_{1,2}$	Heat of solution of cement, KJ/kg
R	Corrected temperature rise, ^{o}C
$W_{i,2}$	Sample weight on ignited basis, g.
T	Ambient temperature, when sample is introduced, ^{o}C
t_d	Final temperature of calorimeter at the end of determination on dry cement, ^{o}C.